Integrating GIS and Green Design Studio to Analyze the Impact of the I-81 Viaduct on Local Communities: Environmental Exposure and Socio-Economic Relationships

Final Report

Authors: Prof. Peng Gao, Prof. Jianshun 'Jensen' Zhang, Prof. Nina Wilson, Prof. Bess Krietemeyer, and Prof. Bing Dong

Organizations: Department of Geography and the Environment (GATE)

Department of Mechanical and Aerospace Engineering (MAE),

School of Architecture (SOA)

Syracuse Center of Excellence (CoE)

Sponsoring Agency: Syracuse University Infrastructure Institute and the School of Architecture

Date: July 31, 2025

Table of Contents

Executive Summary

This report describes a signature research project supported by the Syracuse University Infrastructure Institute (SUII) and the School of Architecture. The project developed a comprehensive research framework to generate policy recommendations for mitigating severe air pollution impacts on vulnerable local communities, specifically addressing air quality concerns related to I-81 viaduct construction in Syracuse.

Project Objectives and Achievements

The research successfully achieved three interconnected objectives:

Objective 1: Air Pollution Prediction. We developed efficient methods to predict spatially and temporally variable air pollution caused by I-81 viaduct construction across the entire city of Syracuse. This was accomplished by combining a CFD-porous model with GIS-based input parameters at the census block group (CBG) scale.

Objective 2: Vulnerable Community Identification. We identified local communities that are both vulnerable to air pollution and experiencing highly concentrated pollution levels. This analysis utilized GIS-based geospatial analysis and geographically weighted regression modeling.

Objective 3: Design Scenario Assessment. We evaluated the potential for air pollution reduction in two representative block sites through five different urban design scenarios, analyzing changes in air quality and thermal conditions for each scenario.

Key Findings

The research revealed that elevated air pollution concentrations would primarily stagnate along the I-81 viaduct corridor, significantly affecting the most vulnerable neighborhoods within this area. Importantly, we demonstrated that deteriorated air conditions in these communities could be substantially improved through appropriate urban renewal strategies.

Implications and Value

The results demonstrate that this new research framework has significant potential to assist policymakers in developing targeted mitigation strategies for the most vulnerable communities experiencing elevated air pollution. The findings also underscore the critical value of interdisciplinary collaboration in addressing complex urban environmental challenges.

This work provides a replicable model for other cities facing similar infrastructure-related air quality challenges, offering both methodological innovation and practical policy guidance for protecting vulnerable populations.

1. Introduction

The New York State Department of Transportation (NYSDOT) launched the Syracuse I-81 viaduct project in July 2023 to remove the elevated Interstate 81 (I-81) viaduct from approximately Colvin Street to Hiawatha Boulevard in the City of Syracuse. The project includes a subsequent community grid initiative that will transform the areas around the former I-81 viaduct into a walkable, human-scaled network of city streets designed to revitalize local communities and improve quality of life.

This transformative infrastructure project presents a unique opportunity to explore new urban renewal frameworks that prioritize community benefit and social responsibility, particularly for neighborhoods with high concentrations of disadvantaged residents. Effective planning requires a holistic vision that considers the interconnected aspects of community well-being: environmental health (specifically air quality), residents' socioeconomic conditions, and the urban built environment. This comprehensive approach demands understanding the spatially variable impacts of air pollution hotspots caused by highway construction on communities with diverse socioeconomic characteristics across different geographic areas, while developing effective planning strategies that can meaningfully improve air quality. Developing such a framework requires expertise across three closely related scientific disciplines: air pollution modeling (environmental engineering), geospatial analysis (geography), and community redesign (architecture).

From an engineering perspective, air pollution from highway construction is well established as a significant public health risk factor (Hoek et al., 2013; Pope et al., 2006). However, new sources of air pollutants can disperse considerable distances—several kilometers—from their origins (Chen et al., 2022; Wu et al., 2017). The complexity of urban built environments, topography, and wind patterns can create concentrated pollution in unexpected neighborhoods with disadvantaged residents who were previously considered safe from air pollution due to their distance from highways (Giovannini et al., 2020; Yu et al., 2023). This potential for widespread dispersion of elevated air pollution necessitates modeling approaches that can rapidly predict spatial distribution of pollutant concentrations across large areas (e.g., entire cities), which exceeds the capacity of conventional urban dispersion models (Antonioni et al., 2012; Pantusheva et al., 2022). New methods are therefore needed to upscale existing computational models.

From a geography perspective, the social fabric of Syracuse has been profoundly shaped by numerous historical urban development patterns, including highway construction (Lane, 2015), resulting in the city having the highest concentration of poverty among the 100 largest US cities (Jargowsky, 2015). The complex interaction between socioeconomic status and public health conditions creates an uneven geographic landscape where neighborhoods in different locations experience varying levels of public health challenges, including diseases caused by air pollution (Clark, 2014). While GIS-

based geostatistical analyses have been widely used to characterize the spatial patterns of various social factors, these methods cannot be directly applied to capture the specific socioeconomic aspects of Syracuse that are most relevant to air pollution vulnerability.

From an architectural perspective, numerous studies have demonstrated relationships between urban building morphologies and air quality, examining how building design can improve air quality in densely built urban environments, particularly through passive strategies that combat the adverse effects of Urban Heat Island (UHI) phenomena (Hassan et al., 2020). The design of building form and spacing can contribute to urban climate resilience (Makvandi et al., 2024), improve environmental quality for pedestrians (Yu & Ma, 2025), and reduce pollutant exposure (Essamlali et al., 2025). Urban canyon conditions, where recirculating vortices often create higher pollutant concentrations (Wang et al., 2025), can be mitigated through strategic introduction of gaps and reconfiguration of building arrays. These interventions allow cleaner air to penetrate lower-velocity, more polluted flow regions, thereby improving urban air quality in outdoor spaces (Liu et al., 2025).

To address these complex challenges across engineering, geography, and architecture, this interdisciplinary research project aims to develop a novel research framework for examining how elevated air pollution from I-81 viaduct construction may disproportionately affect communities with higher percentages of disadvantaged populations, and for assessing the effects of different community planning scenarios on improving air quality. The framework is applied to two representative communities selected along the I-81 corridor. The research has accomplished three primary objectives:

Objective 1: Developed a predictive model for spatial air pollution distribution throughout Syracuse by integrating GIS-based urban morphology data, field-measured air quality data, and porous medium computational fluid dynamics (CFD) modeling.

Objective 2: Identified communities in census block groups with high percentages of disadvantaged population that experience disproportionately severe air pollution impacts.

Objective 3: Assessed the improvement of air quality in two severely affected local communities based on five different architectural redesign plans.

2. Methodology

This study employs a systematic approach consisting of three interrelated modules to address the research goal (Fig. 1).

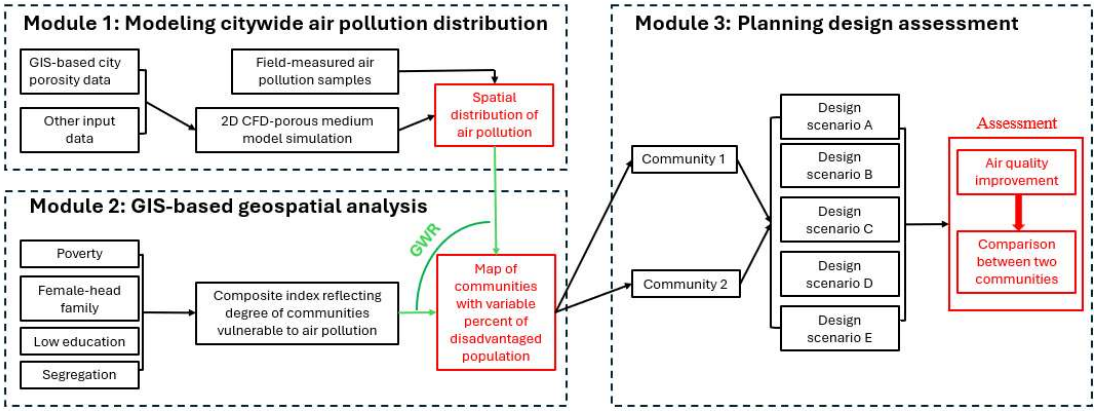

Figure 1. The workflow of the developed comprehensive approach.

2.1. Module 1: Modeling citywide air pollution distribution due to highway construction

Module 1 features computer-modeling of air pollution exposures across the entire city of Syracuse. We adopt a 2D CFD-porous medium model for achieving this goal. At the

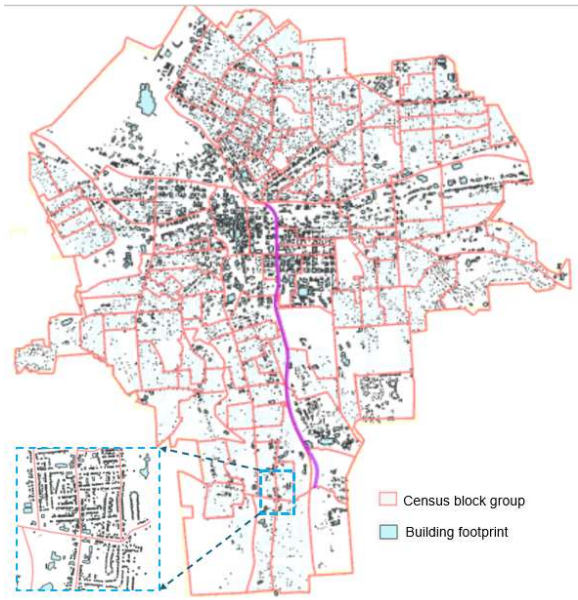

Figure 2. The study area (Syracuse) with census block groups and building footprints. The north-south oriented purple line is the I-81 viaduct.

city scale, model simulations are inherently complex because of the geometric diversity and density of buildings across the city. In Syracuse, our area of interest, there are

approximately 51,865 buildings bounded by 133 census block groups, the spatial unit this project is based on (Fig. 2). Each building has a unique and often intricate geometry, which presents significant challenges for conventional modeling approaches. Therefore, a simplified modeling strategy, termed a porous medium approach, is adopted in this study. The core of this approach is that the spatial properties of buildings within each CBG is represented by a value of the parameter originally used to characterize urban morphology, porosity (Adolphe, 2001). In this study, the porosity (ε) is defined as

$$\varepsilon = \frac{A_{open}}{A_{total}} \tag{1}$$

where A_{open} is the total open areas among buildings and A_{total} is the total area of the CBG within which these buildings are located (Fig. 3a). In reality, the buildings are separated by major roads, which play an important role in determining airflow dynamics because they are primary flow channels (Fig. 3b). Values of porosity for all 133 CBGs

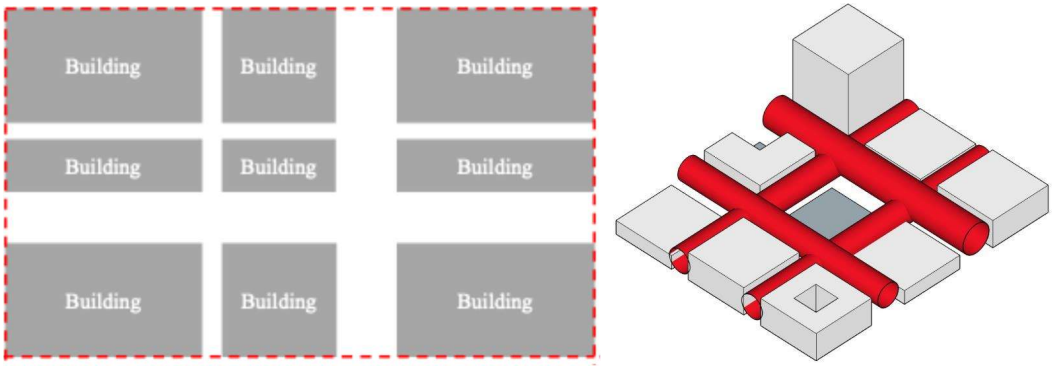

(a) (b)

Figure 3. The concepts of porosity and airflow in urban morphology. (a) the geometric illustration of porosity in a CBG, (b) streets as the main airflow channels.

and the street network are calculated and developed in ArcGIS platform.

In the CFD model, the pressure gradient in the x-direction ($\frac{dP}{dx}$) equals the source term (S_i), which is the negative sum of two components including viscous and inertia loss term.

$$\frac{dP}{dx} = S_i = -\left(\sum_{j=1}^{3} D_{ij}\mu v_j + \sum_{j=1}^{3} C_{ij}\frac{1}{2}\rho|v|v_j\right) \tag{2}$$

where $D_{ij}$and $C_{ij}$are the viscous and inertial resistance coefficients, respectively. μ is the dynamic viscosity. ρ is the fluid density, and v_j is the velocity component in the j-th direction. Next, pressure drop can be also calculated based on Ergun equation which is the following equation.

$$\Delta p = \frac{150\mu L}{D_p^2} \cdot \frac{(1-\epsilon)^2}{\epsilon^3} v_s + \frac{1.75 L\rho}{D_p} \cdot \frac{(1-\epsilon)}{\epsilon^3} v_s |v_s| \quad (3)$$

where, L represents the length of the porous medium in the flow direction. D_p is the diameter of the particles in the porous medium, and v_s is superficial velocity.

By comparing with Eqn. (2) and (3), viscous and inertial loss terms are calculated as following equations

$$D_{ij} = \frac{150}{D_p^2} \frac{(1-\varepsilon)^2}{\varepsilon^3} \quad (4)$$

$$C_{ij} = \frac{2 * 1.75}{D_p^2} \frac{(1-\varepsilon)}{\varepsilon^3} \quad (5)$$

In this study, D_p is to be 30 m^3, when assume building volume is about 11,327–14,158 m^3. From eq. (2) – (5), it can be seen that porosity at the CBG level is a key input parameter serving as a simplified 'porous medium' in the domain (i.e., the city of

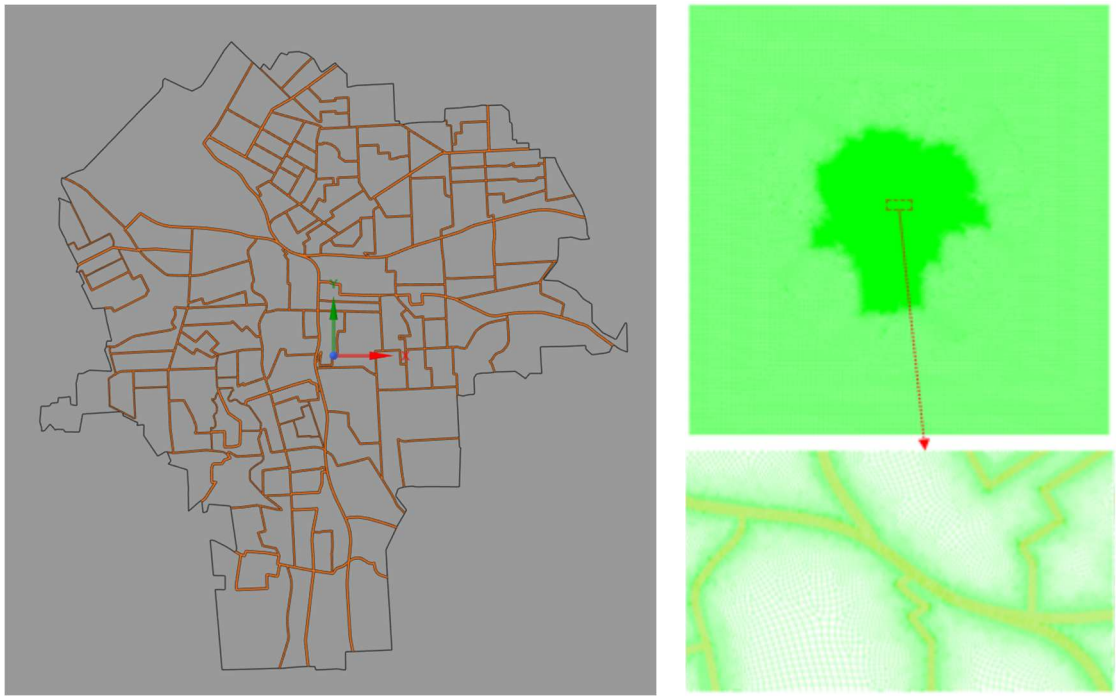

(a) (b)

Figure 4. Illustration of the computational domain in the CFD model. (a) boundaries of CBGs, (b) a non-uniform mesh.

Syracuse) of the CFD simulation to represent the aggregated impact of buildings at the CBG level on air flows. Thus, the CBGs and the associated street network constitute the computational geometry used for the simulation of airflow and pollutant dispersion at the urban scale (Fig. 4a). Each CBG is assigned a porosity value calculated based on its

enclosed building geometries for representing building-induced resistance to airflow. In reference to these simplified physical urban structures, a non-uniform mesh is created as the computational domain with finer-resolution grids used along streets to ensure correct representation of the main airflow channels (Fig. 4b).

As another important input parameter, weather data in 2024, including monthly averaged wind speed and wind direction probabilities, are collected from the online pen source (https://weatherspark.com/y/22184/Average-Weather-in-Syracuse-New-York-United-States-Year-Round#google_vignette). These data are input in the CFD model to perform simulations for each month using the corresponding average inlet wind velocity. For each month, four simulations are performed to represent four prevailing wind directions.

From the CFD simulation outputs, the aera averaged air pollutant concentration in each CBG is calculated under each wind direction. These values are then averaged over the four directions weighted by the wind direction probabilities to obtain the monthly average pollution concentration for each CBG. For the purposes of the subsequent analysis in Module 2, the monthly data are finally aggregated to produce annually averaged pollution concentrations for year-round assessment (C_{ap}) the red box within Module 1 in Fig. 1).

2.2. Module 2: GIS-based geospatial analysis

Module 2 employs GIS-based geospatial analysis to identify socioeconomically disadvantaged local communities and examine the spatial relationship between their distribution and increased air pollution resulting from I-81 viaduct construction (Fig. 1). Air pollution, as a critical public health issue, is closely interconnected with the socioeconomic status of urban residents.

This study examines four social determinants of public health that are potentially most relevant to air pollution exposure and health outcomes. Poverty is measured as the percentage of the population living below the national poverty threshold. Vulnerability represents the percentage of the population under age 14 or over 65, groups typically more susceptible to air pollution health effects. Segregation is defined as the percentage of Black and minority residents in a community. Distance to Medical Resources (DMR) measures the distance from each census block group (CBG) centroid to the nearest available medical facility.

Each factor is calculated for all 133 CBGs covering Syracuse as spatially aggregated values. The analysis is conducted using the ArcGIS platform, and the resulting maps display the spatial distribution of each factor across the city. This approach enables the identification of areas where socioeconomic disadvantage may compound the health risks associated with transportation-related air pollution.

Preliminary analysis reveals that these four socioeconomic factors exhibit distinct and non-overlapping spatial patterns, reflecting the multifaceted nature of social disadvantage

in Syracuse. This spatial complexity makes it challenging to directly assess relationships between individual factors and the air pollution concentrations predicted in Module 1. To address this analytical challenge, the four factors must be integrated into a unified measure that captures overall socioeconomic vulnerability to air pollution at the CBG level. Therefore, this study develops a composite socioeconomic indicator (I_s) that synthesizes vulnerability to air pollution across multiple dimensions of social disadvantage. The indicator integrates the four selected social determinant factors through a weighted linear aggregation model, creating a comprehensive measure that accounts for the cumulative effects of poverty, demographic vulnerability, racial segregation, and healthcare accessibility on air pollution exposure risk. The model is expressed as follows (Malczewski, 1999):

$$I_s = \sum_{i=1}^{n} \omega_i \cdot x_i \quad (6)$$

where n is the number of the factors, which is 4, ω_i is the weight assigned to each factor i, x_i is the normalized value of factor i. The sum of the weights is equal to 1 ($\sum_{i=1}^{n} \omega_i = 1$) to maintain a consistent and interpretable scale for the calculated index. To optimize the weighting scheme, we conduct sensitivity analysis using Monte Carlo simulations, selecting weights that minimize variability in the final I_s values. Calculating I_s for all 133 CBGs in ArcGIS platform leads to a map showing the spatial distribution of local communities with different degrees of vulnerability to air pollution (the middle box in Module 2 in Fig. 1).

The geospatial relationship between vulnerable local communities and elevated air pollution is examined through two complementary analytical approaches.

First, a direct spatial comparison is conducted between the composite socioeconomic vulnerability patterns and the air pollution concentration maps generated in Module 1. This overlay analysis produces a combined classification map that categorizes CBGs according to their intersection of socioeconomic vulnerability levels (low, medium, high) and air pollution concentrations (low, medium, high). The resultant map enables the identification of CBGs experiencing both medium-to-high socioeconomic vulnerability and medium-to-high air pollution concentrations, representing communities that bear a disproportionate burden from I-81 viaduct construction. These areas can be classified as environmental justice concern zones where transportation infrastructure negatively impacts already disadvantaged populations.

However, spatial overlay analysis alone cannot determine whether a statistically significant correlation exists between the degree of socioeconomic vulnerability and air pollution concentration levels across CBGs. While this approach effectively identifies geographic coincidence of disadvantage and pollution exposure, it does not establish the strength or statistical significance of the relationship between these variables.

Second, we performed geographically weighted regression (GWR) between the index I_s and C_{ap}. The GWR fits a separate regression equation at each location in the dataset, weighting nearby observations more heavily than distant ones. It helps explore how the

strength, direction, and significance of relationships change over space. Mathematically, a GWR model is (Fotheringham, et al., 2002)

$$y_i = \beta_0(u_i, v_i) + \sum_{k=1}^{p} \beta_k(u_i, v_i) x_{ik} + \varepsilon_i \quad (7)$$

where (u_i, v_i) are spatial coordinates of location i, $\beta_k(u_i, v_i)$ is location-specific regression coefficients, x_{ik} is the independent variables, which in this study contain one variable, C_{ap}, and y_i is the dependent variable, which is I_s in this study. The GWR accounts for the effect of spatial autocorrelation and identifies statistically significant correlations between the two variables for CBGs. The results allow for generating the final map indicating more vulnerable local communities that may suffer medium or high degree of air pollution (the red box in Module 2 in Fig. 1).

2.3. Module 3: Planning design assessment

Module 3 highlights different architectural design scenarios that could improve air quality in different ways for the most affected local communities with higher degrees of vulnerability (Fig. 1). Based on the final map obtained from Module 2, we selected two representative local communities along the I-81 viaduct that are not only more vulnerable to air pollution but also would suffer elevated high air pollution concentrations. For each of the two sites, morphological characteristics of building density and spacing were altered to improve the sites' access to fresh air and higher-velocity airflow based on prevailing warm-weather seasonal wind conditions when natural ventilation and outdoor occupied spaces are activated the most. We designed five different scenarios:

- Configuration A is proposed to reduce the built density of the block by reducing the footprint of the buildings to facilitate the passage of fresh air in between horizontal rows of buildings.
- Configuration B illustrates a modification in building rugosity in the proportion of building height regularity, thus changing the surface roughness of the landscape and altering the original skimming flow condition.
- Configuration C also reduces building density, but building heights are staggered between two and four stories in the west-east direction, perpendicular to prevailing breezes, in order to increase site rugosity and attempt to reduce the effects of skimming flow typically found in arrangements having many rows of buildings of a very similar height.
- Configuration E is proposed to subtract staggered built areas within the densely-built housing block so that ventilation and occupied green spaces can contribute microclimatic benefits mitigating the Urban Heat Island conditions by cooling air and removing pollutants.

For each selected site, solar radiation distributed on the top of buildings is calculated and wind pathways with unhealthy, average, and good air quality are determined in the plan view of the site and along a representative vertical profile. These results serve as the benchmark for comparison with each of the five new planning design scenarios.

3. Results

Our comprehensive analyses generate a diverse array of cartographic visualizations and analytical outputs presented in multiple formats, successfully fulfilling each of the three research objectives established at the outset of this study. These deliverables encompass detailed spatial maps, quantitative datasets, statistical summaries, and interpretive findings that collectively address the core research questions while providing stakeholders with accessible and actionable insights across different presentation modalities.

3.1. Results relevant to objective 1 (Module 1)

The CFD model predictions depend on the input wind data. The average wind speeds are used as boundary conditions in the CFD simulations, and the wind direction

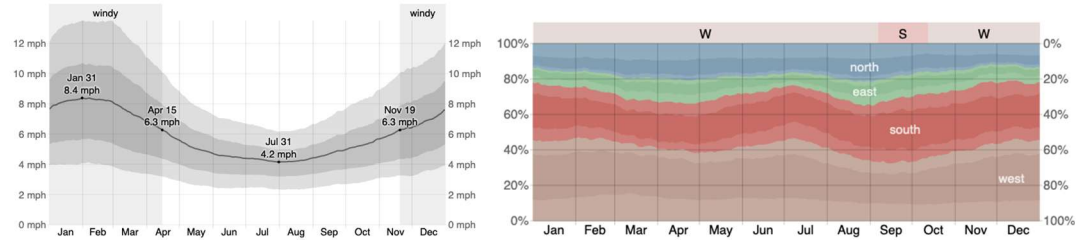

(a) (b)

Figure 5. The 2024 wind patterns in Syracuse. (a) average wind speed, and (b) wind direction probabilities.

Table 1 Syracuse Average Wind Speed and Wind Direction Probability

Variables	Jan	Feb	Mar	Apr	May	Jun	Jul	Aug	Sep	Oct	Nov	Dec
Average Wind Speed (mph)	8.1	8.3	7.4	6.2	5.1	4.5	4.3	4.3	4.7	5.3	6.1	7
North Wind Probability (%)	14.7	16.7	19.2	20.4	19.5	17.4	17.2	20.6	18.7	16.4	13.5	12.4
South Wind Probability (%)	30.6	27.4	25.3	25.5	29	30.2	30	30.5	35.2	35.5	34.9	33.2
West Wind Probability (%)	46.5	46.4	43.3	40.8	40.4	43.7	44.7	37.1	33.5	36	40.9	45.9
East Wind Probability (%)	8.2	9.5	12.2	13.3	11.1	8.7	8.1	11.8	12.6	12.1	10.7	8.5

probabilities are incorporated into the post-processing stage to calculate monthly-averaged contaminant concentrations weighted by directional frequency. The monthly averaged wind patterns (speed and direction probabilities) are summarized in **Error!**

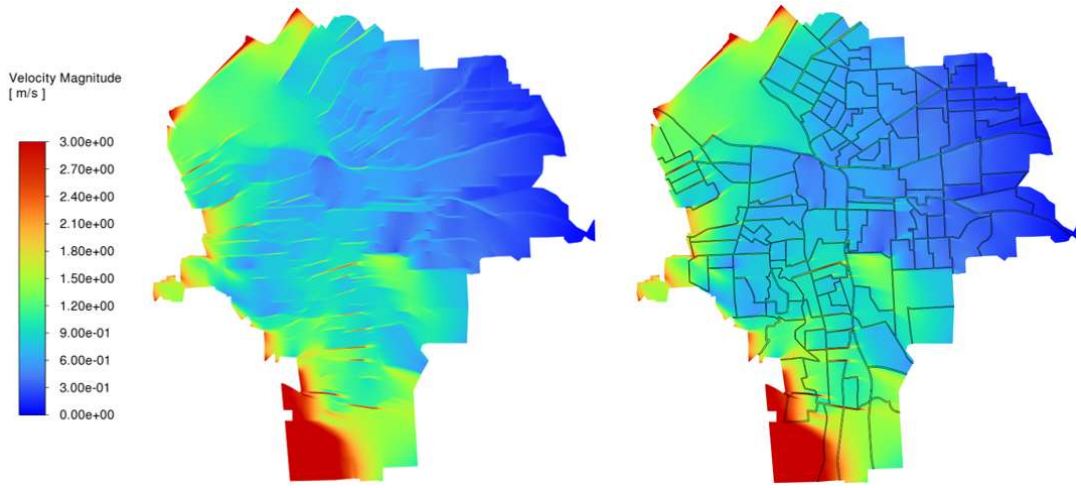

(a) (b)

Figure 6. Modeled wind velocity distributions under pure west wind. (a) without street boundaries, and (b) with street boundaries.

Reference source not found., while the corresponding monthly averaged wind speed values are listed in Table 1. In general, summer winds are minor, whereas winter winds are strong. Over a year, winds in Syracuse mostly come from west.

Our first step is to test the model performance by using single-direction wind patterns as the input data. Figure 6 presents the airflow velocity distribution in the city under west wind conditions. As expected, the western part of the city experiences relatively high flow velocities. 6(a) and (b) display the same velocity field, but 6(b) includes the street boundaries. By comparing these two subfigures, the flow channeling effect becomes evident, particularly along regions where major streets are aligned parallel to the wind direction. These roads act as low-resistance pathways that enhance airflow penetration. The spatial variations of the airflow velocities also reflect the spatially uneven effect of buildings as surface roughness.

Error! Reference source not found.7 shows the airflow velocity distribution under north wind conditions. A similar trend is observed, with noticeable flow enhancement along major roadways that align with the incoming wind direction. Both simulation outcomes indicate that the CFD model with the simplified computational structure can predict air flow distribution over a large spatial scale (i.e., the entire city) well.

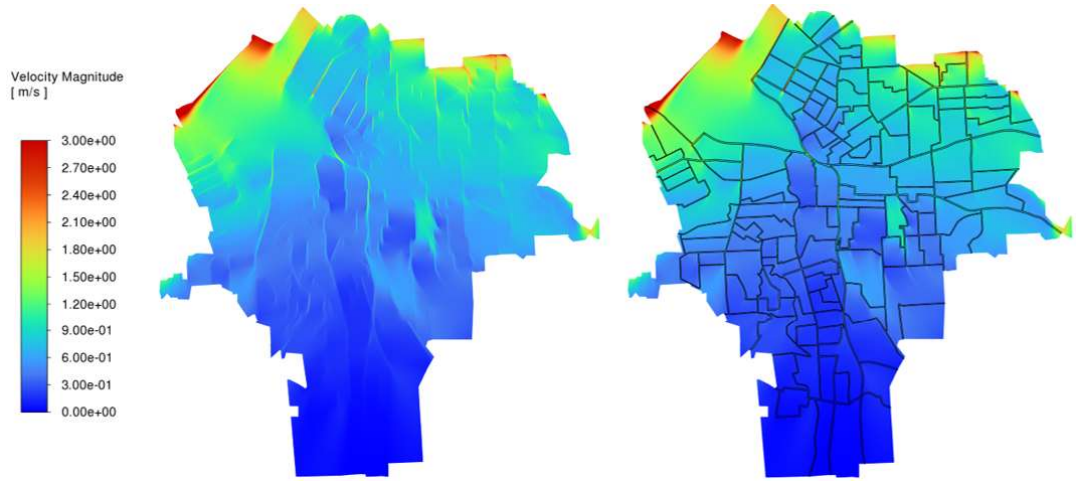

(a) (b)

Figure 7. Modeled wind velocity distributions under pure north wind. (a) without street boundaries, and (b) with street boundaries.

In the second step, we simulated the dynamics of pollutants ($PM_{2.5}$) emitted from highway I-81 and I-690 driven by the west and north wind, respectively. The emission from I-81 reflect the elevated air pollution due to the I-81 viaduct construction. Under the west wind conditions (Fig. 8a), elevated concentrations are observed in the eastern part of the city, indicating the transport of pollutants from west to east. Notably, the northeastern area experiences the highest pollutant levels, where the intersect of the two highways near the city center, results in a localized buildup of pollutants, suggesting that wind is

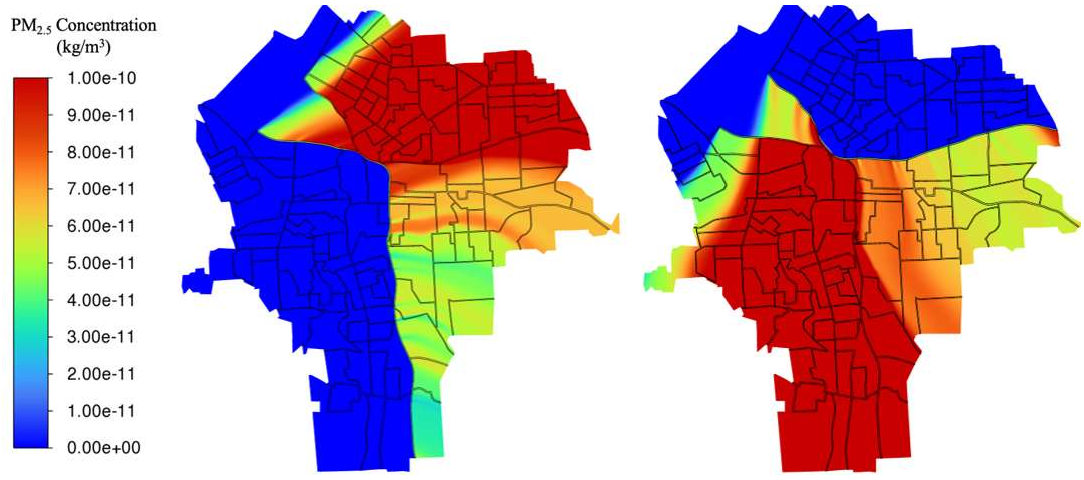

(a) (b)

Figure 8. The predicted spatial distribution of pollutants ($PM_{2.5}$) under two different prevailing winds. (a) west wind, and (b) north wind.

the sole driving force determining the spatial distribution of pollutants. Under the north

wind conditions (Fig. 8b), the concentration pattern shifts southward, with particularly high levels in the southwestern region, consistent with the direction of incoming airflow. These results underscore the significant influence of wind direction on pollutant dispersion and the spatial variability of air quality at the neighborhood scale.

Next, we predicted the spatial distribution of monthly averaged pollutant concentrations for July 2024. The result (Fig. 9a) represents the weighted average across four simulated wind directions using the average wind speed for that month. It is evident that CBGs located near major highways, I-81 and I-690, exhibit higher pollutant concentrations, shown in shades of red and orange. These elevated values reflect the localized impact of traffic emissions and limited ventilation in the densely built environments. In contrast, areas farther from major roadways generally show lower concentrations, suggesting better air circulation or reduced source proximity. Finally, we calculated area-averaged pollutant concentrations for each CBG under different wind speeds and four principal wind directions in each month. Then, we computed for each CBG wind-direction-weighted average pollutant concentrations for every month in 2024. Based on these values, we computed the annual average air pollution concentrations for

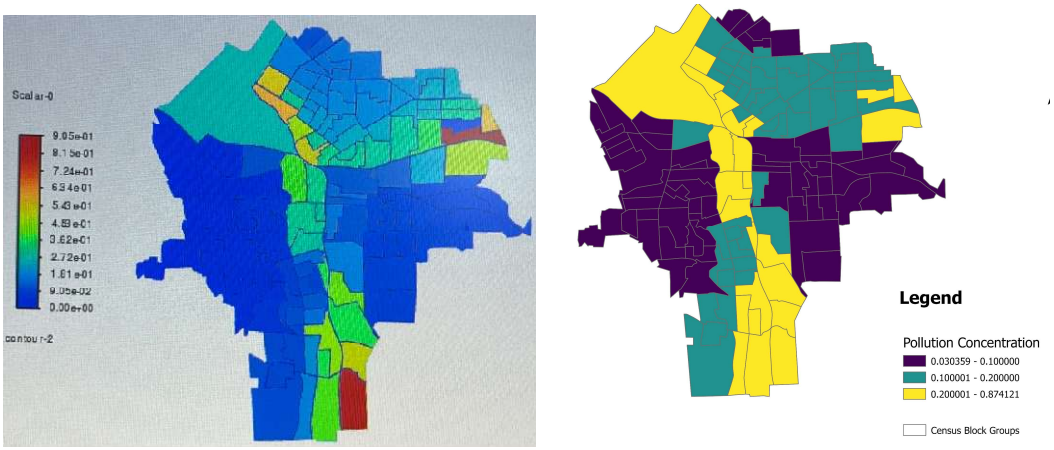

(a) (b)

Figure 9. Spatial distributions of time-averaged pollutant concentrations. (a) July 2024, and (b) the whole year of 2024. The values are aggregated in CBGs and presented using Jenks's classification method, which minimizes the variance within each class, while maximizing the between-class variance.

133 CBGs in Syracuse (Fig. 9b). These values exhibit an interesting spatial distribution. Local communities close to the I-81 viaduct would generally experience high degrees of elevated air pollution. For the northern section of the I-81 viaduct, the surrounded CBGs on both sides would have high air pollution concentrations, but CBGs on the west side of the southern section of the I-81 viaduct may experience medium degrees of air pollution. It appears that the elevated air pollution along the I-81 viaduct due to construction tends to linger around its source zones, though wind direction changes annually. This suggests

that neighborhoods near the I-81 viaduct are the main area adversely affected by elevated air pollution from the highway construction.

3.2. Results relevant to objective 2 (Module 2)

3.2.1. Geospatial patterns of social determinant factors and the composite index

<u>The four individual factors</u>

The spatial distributions of the four selected socioeconomic factors exhibit distinctly

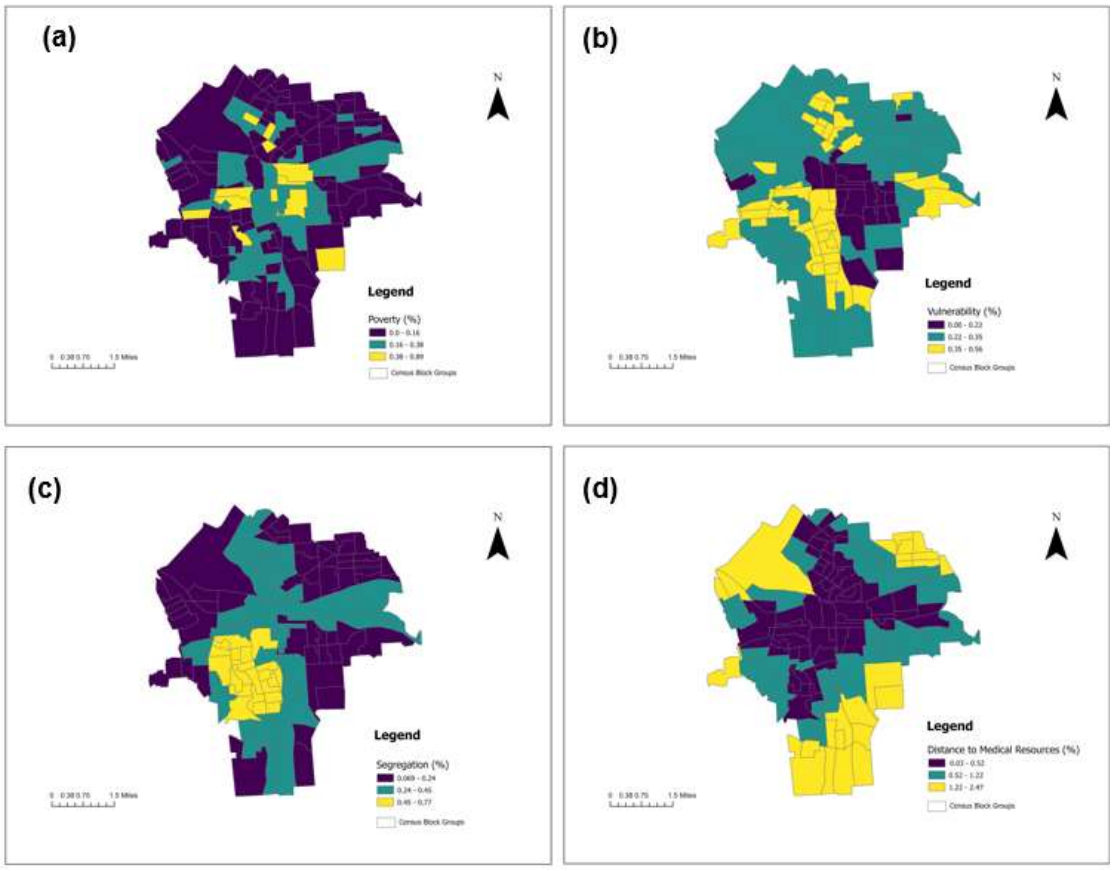

Figure 10. Spatial distribution of the four selected social determinant factors. (a) Poverty; (b) Vulnerability; (c) Segregation; (d) Distance to Medical Resources. The classification method of each map is the same as in Figure 9.

different patterns across the study area, revealing complex geographic variations in urban social conditions (Fig. 10). Poverty concentrations follow a centralized pattern with directional extensions. Census block groups (CBGs) with medium and high percentages of population in poverty are predominantly clustered in the city geometric center, forming a core area that extends outward in narrow corridors toward all four cardinal directions (Fig. 10a). Notably, this poverty distribution does not align with the north-south orientation of the I-81 viaduct corridor, suggesting that transportation infrastructure

alone does not determine poverty geography.

Air pollution vulnerability displays a markedly different spatial arrangement, with a strong association to major transportation corridors. A substantial proportion of CBGs with high vulnerability to air pollution are concentrated within and immediately adjacent to the western side of the I-81 viaduct corridor (Fig. 10b). Additional high-vulnerability areas are scattered toward both the western and eastern city boundaries, as well as in northern sections of the study area. The majority of local communities fall into the medium vulnerability category, creating a buffer zone between high-vulnerability areas and lower-risk neighborhoods.

Segregation patterns reveal a pronounced southwestern concentration. Neighborhoods experiencing high segregation rates form a dense cluster extending from the geometric center of the city toward the southwest, reaching approximately halfway to the southern city boundary (Fig. 10c). This high-segregation core is encircled by areas with medium segregation rates that radiate outward and extend to the city boundaries in multiple directions, creating a gradient effect from the central concentration.

Access to medical resources shows a distinct southern concentration of disadvantage. Residents facing the longest travel distances to medical resources (DMR) are primarily located in CBGs clustered near the southern city boundary (Fig. 10d). In contrast, communities with shorter distances to medical resources form an extensive zone that occupies the city center and extends outward in belt-like formations, providing better healthcare accessibility to central and north-central residents.

These divergent spatial patterns among the four factors demonstrate that the geographic characteristics of socioeconomic status in urban environments are highly complex and multifaceted, even when analyzed at the relatively aggregated spatial scale of census block groups. The distinct and non-overlapping spatial patterns of these socioeconomic indicators highlight the need to develop a composite index that captures the combined and potentially synergistic effects of multiple factors operating simultaneously across the urban landscape.

The composite index

The spatial distribution of the composite vulnerability index (*I*s) reveals a pronounced bi-polar geographic pattern across the study city, with distinct clustering characteristics that reflect underlying socioeconomic and environmental disparities. Census block groups (CBGs) exhibiting the highest vulnerability scores are predominantly concentrated along the southern corridor of the city, forming a continuous zone of elevated risk that encompasses the entire length of the I-81 viaduct infrastructure. This southern concentration represents a zone of heightened environmental justice concern, where multiple vulnerability factors converge to create compounded risks for resident populations.

In contrast, CBGs characterized by medium and low vulnerability values demonstrate

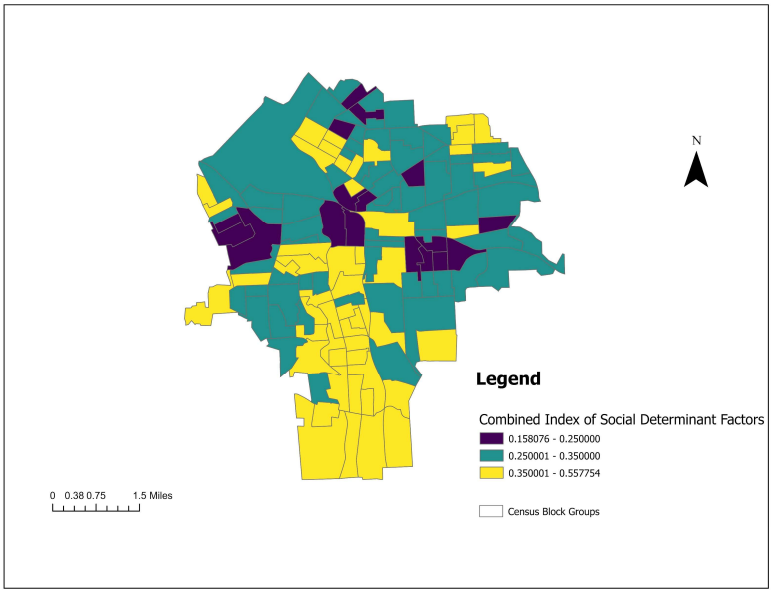

Figure 11. The spatial distribution of the I_S values over the city. The classification method is the same as in Figure 9.

a clear spatial preference for the northern portions of the city, positioned beyond the immediate influence zone of the I-81 viaduct (Fig. 11). This geographic bifurcation suggests that the transportation infrastructure serves not only as a physical barrier but also as a demarcation line between areas of varying socioeconomic resilience and environmental burden.

This spatial pattern reveals that local communities situated in close proximity to the I-81 viaduct consistently demonstrate elevated degrees of vulnerability to air pollution exposure and related environmental health risks. These vulnerable communities are not confined to the immediate vicinity of the transportation corridor but exhibit a notable spatial extension pattern, particularly toward the southern terminus of the city. The persistence and geographic extent of these vulnerability patterns indicate that air pollution impacts extend well beyond the immediate footprint of the transportation infrastructure, creating zones of environmental injustice that affect broader residential neighborhoods and communities throughout the southern urban landscape.

3.2.2. Geospatial relationships between elevated air pollution and the composite index

Direct comparison

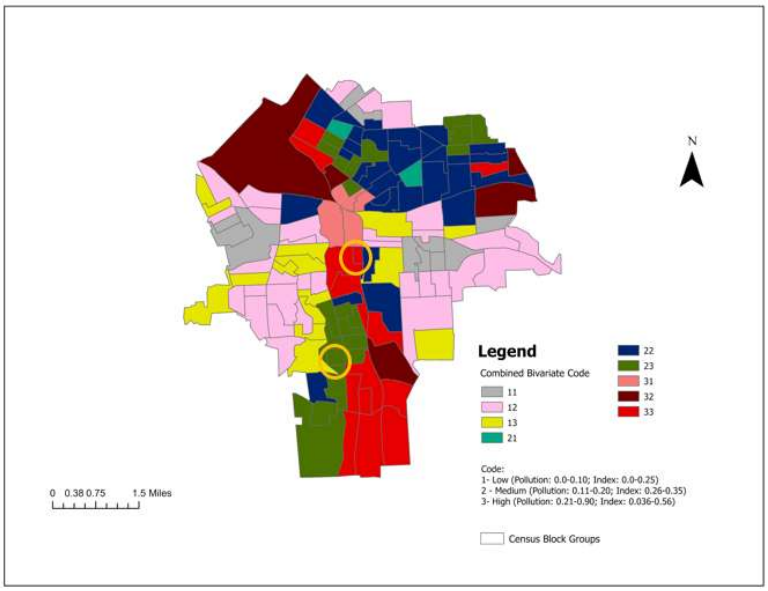

Figure 12. The geospatial relationship between the composite index and the elevated air pollution. The first number next to each color represents the class of pollution concentration, while the second reflects the class of the index. For example, a CBG with '23' (i.e., dark green) means this CBG has a medium value of pollution concentration and high value of the index. The two CBGs marked by orange circle include the two sites selected for redesign analysis in section 3.3.

A comprehensive spatial comparison between the composite vulnerability index and predicted air pollution concentrations reveals critical environmental justice patterns and establishes clear spatial relationships at the CBG level (Fig. 12). This comparative analysis employs a dual-classification system where each CBG receives a two-digit designation: the first digit represents the vulnerability index category, and the second digit indicates the air pollution concentration level, with higher numbers signifying greater vulnerability and pollution exposure, respectively. CBGs designated with classification codes containing either '2' or '3' in both positions represent local communities that face a dual burden of medium to high vulnerability to air pollution impacts while simultaneously experiencing medium to high actual pollution concentrations due to the I-81 viaduct construction. This combination of high vulnerability and high exposure creates compounded environmental health risks that disproportionately affect these residential areas, highlighting critical zones where social susceptibility intersects with environmental hazard exposure.

The most concerning areas are represented by CBGs classified as '33' (depicted in red in Fig. 12), which constitute neighborhoods facing the most severe environmental justice challenges. These communities exhibit the highest vulnerability to air pollution impacts while simultaneously enduring the most elevated pollution concentrations, creating a

"perfect storm" of environmental health risk. Spatially, these critically affected areas demonstrate a distinct clustering pattern along the eastern corridor of the southern section of the I-81 viaduct, with additional isolated pockets extending sporadically northward along the transportation infrastructure (Fig. 12). The concentration of these highest-risk communities in proximity to major transportation infrastructure suggests a direct relationship between highway emissions, local air quality degradation, and the residential patterns of vulnerable populations. These neighborhoods represent the highest priority areas for immediate intervention and should receive primary focus in any comprehensive environmental health mitigation strategy.

Additionally, CBGs classified as '23' (depicted in dark green in Fig. 12) represent communities that, while possessing relatively better socioeconomic resilience compared to the '33' areas, still face significant environmental health challenges due to high air pollution exposure. These areas demonstrate that environmental burden can affect communities across different socioeconomic strata, though the capacity to cope with and adapt to these exposures may vary. Geographically, these moderately vulnerable but highly exposed communities are predominantly distributed along the western corridor of the southern section of the I-81 viaduct, creating a complementary pattern to the eastern concentration of highest-risk areas. This spatial distribution suggests that the transportation infrastructure creates a zone of elevated pollution exposure that affects communities on both sides of the corridor, though the social vulnerability characteristics differ between eastern and western residential areas.

The identification of both '33' and '23' communities as priority areas underscores the need for a comprehensive, spatially targeted mitigation approach that addresses both the sources of pollution exposure and the underlying social factors that contribute to vulnerability. These findings demonstrate that effective environmental health interventions must consider not only pollution reduction strategies but also community-specific resilience-building measures that account for varying socioeconomic capacities and environmental health risks across different neighborhood contexts.

Geographically weighted regression analysis

Figure 13. Geospatial relationships between the composite index and pollution concentrations identified from geographically weighted regression analysis. (a) CBGs with statistically significant correlations; (b) the dual-classes of the two variables in these CBGs.

While the geospatial relationships observed in CBGs and illustrated in Figure 8 provide valuable insights into the spatial co-occurrence of vulnerability and pollution exposure, these visual patterns alone may not constitute statistically robust evidence of causal or correlational relationships. To address this analytical limitation and establish more rigorous empirical foundations for our findings, we employed Geographically Weighted Regression (GWR) modeling to identify CBGs where the relationship between socioeconomic vulnerability and air pollution concentrations demonstrates statistical significance at the local level (Fig. 13a).

The GWR analysis reveals important spatial heterogeneity in the strength and significance of these relationships across the study area. Notably, the correlation coefficients among the statistically significant CBGs exhibit considerable variation, indicating that the strength of the vulnerability-pollution relationship fluctuates spatially across different neighborhoods and community contexts. While this variation in correlation magnitudes represents an important dimension of spatial heterogeneity that merits future investigation, the present study prioritizes the identification of areas where statistically significant relationships exist, regardless of the specific strength of those correlations. This analytical approach focuses on establishing the presence of meaningful statistical associations rather than quantifying their relative magnitudes, as the existence of significant relationships provides the foundational evidence necessary for targeted intervention strategies.

The spatial distribution of statistically significant CBGs demonstrates a pronounced concentration in the central and southern portions of the city, with notable extensions that reach well beyond the immediate vicinity corridor of the I-81 viaduct infrastructure (Fig. 13a). This expanded geographic footprint suggests that the influence of transportation-related air pollution on community vulnerability operates across a broader spatial scale than might be anticipated from proximity analysis alone. The majority of these

statistically significant CBGs located on the southern side of the city correspond directly to the high-priority areas previously identified through visual analysis in Figure 12, providing statistical validation for the spatial patterns observed in the earlier descriptive analysis (Fig. 13b).

The spatial distribution of statistically significant CBGs demonstrates a pronounced concentration in the central and southern portions of the city, with notable extensions that reach well beyond the immediate vicinity corridor of the I-81 viaduct infrastructure (Fig. 13a). This expanded geographic footprint suggests that the influence of transportation-related air pollution on community vulnerability operates across a broader spatial scale than might be anticipated from proximity analysis alone. The majority of these statistically significant CBGs located on the southern side of the city correspond directly to the high-priority areas previously identified through visual analysis in Figure 12, providing statistical validation for the spatial patterns observed in the earlier descriptive analysis (Fig. 13b).

The presence of statistically significant correlations in these southern CBGs carries profound implications for understanding the causal mechanisms underlying environmental health disparities. These statistical relationships suggest that the vulnerable socioeconomic status of residents in these neighborhoods is not merely coincidentally co-located with elevated air pollution, but rather may be causally influenced by the persistent exposure to elevated pollution concentrations sourced primarily from I-81 highway emissions. Furthermore, the anticipated construction activities associated with the I-81 viaduct replacement project, which are expected to temporarily worsen air pollution conditions in these areas, could potentially trigger a cascading effect that pushes these already vulnerable communities toward even more precarious socioeconomic circumstances.

This statistical validation has critical implications for understanding community resilience and adaptive capacity across different neighborhood contexts. In contrast to the statistically significant CBGs, other communities that exhibit similar dual-classification patterns (represented by the red and dark green areas in Figure 12) but lack statistically significant vulnerability-pollution correlations appear to possess greater resilience to air quality fluctuations. The vulnerable status in these non-significant areas may be driven by factors other than air pollution exposure, such as historical disinvestment, structural racism, or other socioeconomic determinants that operate independently of environmental quality variations.

Therefore, our GWR results provide empirical support for the hypothesis that targeted mitigation strategies designed to improve air pollution conditions could generate measurable improvements in the socioeconomic status and overall well-being of residents in the identified statistically significant CBGs, particularly those concentrated on the southern side of the city. This finding suggests that environmental interventions in these areas may yield dual benefits: direct health improvements through reduced pollution

exposure and indirect socioeconomic improvements through enhanced community stability and reduced environmental stress. Conversely, communities where vulnerability and pollution are not statistically correlated may require alternative intervention approaches that address the underlying non-environmental drivers of social vulnerability, such as housing policy, economic development, or infrastructure investment strategies that operate independently of air quality improvements.

3.3. Results relevant to objective 3 (Module 3)

We selected two sites within the corridor of the I-81 viaduct, Pioneer Homes (red dot) and Matson Ave (blue dot) (Fig. 14). Site 1 (Pioneer Homes) belongs to the community subject to the most severe environmental justice challenges, while site 2 is a part of the CBG with better socioeconomic resilience, but still suffering from significant air pollution (Fig. 12). Furthermore, the air pollution condition in site 1 is independent of its socioeconomic status, whereas in site 2, it is the main driving force for its socioeconomic status. Thus, the same change of air pollution conditions in the two sites could have different impact on their socioeconomic status.

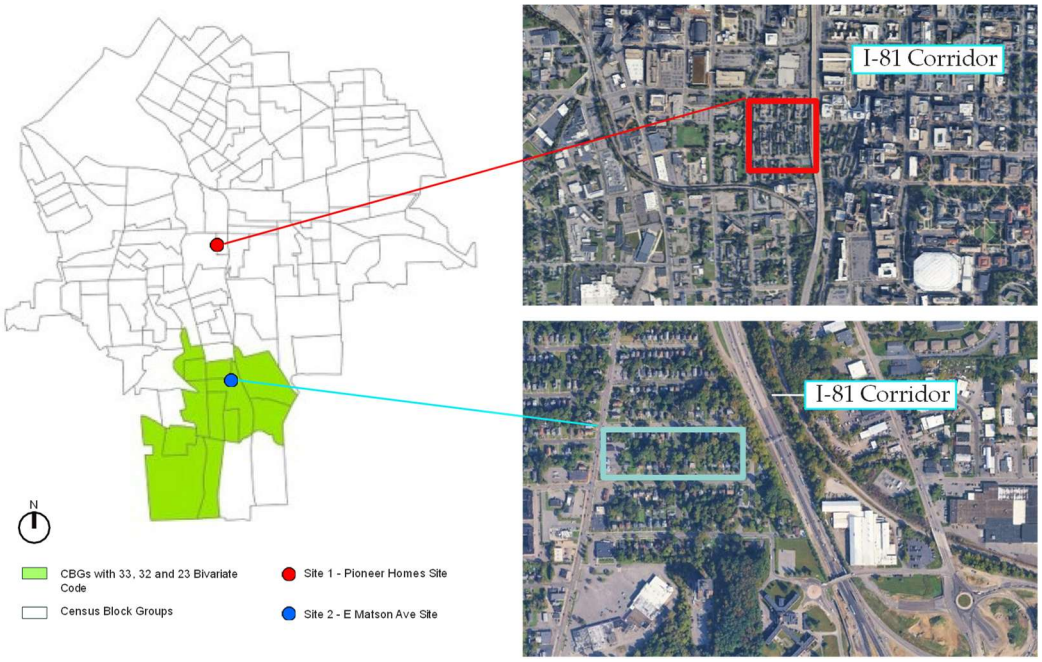

Figure 14. Locations of the two selected sites for redesign analysis

3.3.1. Site 1: Pioneer Homes

Pioneer Homes is Syracuse's oldest public housing project, built in 1942. The development consists of low-rise brick masonry buildings shaped like bars or L's. Each building contains three to five units, and the buildings are positioned close together along the north-south axis. This tight spacing creates air circulation problems. The arrangement blocks westerly and northwesterly summer breezes (Fig. 15) from moving between building rows. The similar building shapes may cause air to skim over the tops rather than circulate down into the spaces between buildings. This prevents fresh air from reaching the ground level areas, which also receive high solar heat. This phenomenon is common in low-rise urban developments and leads to poor air quality with high pollutant concentrations in the spaces between buildings.

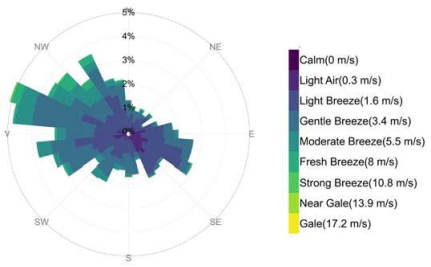

Figure 15. The wind pattern in summers

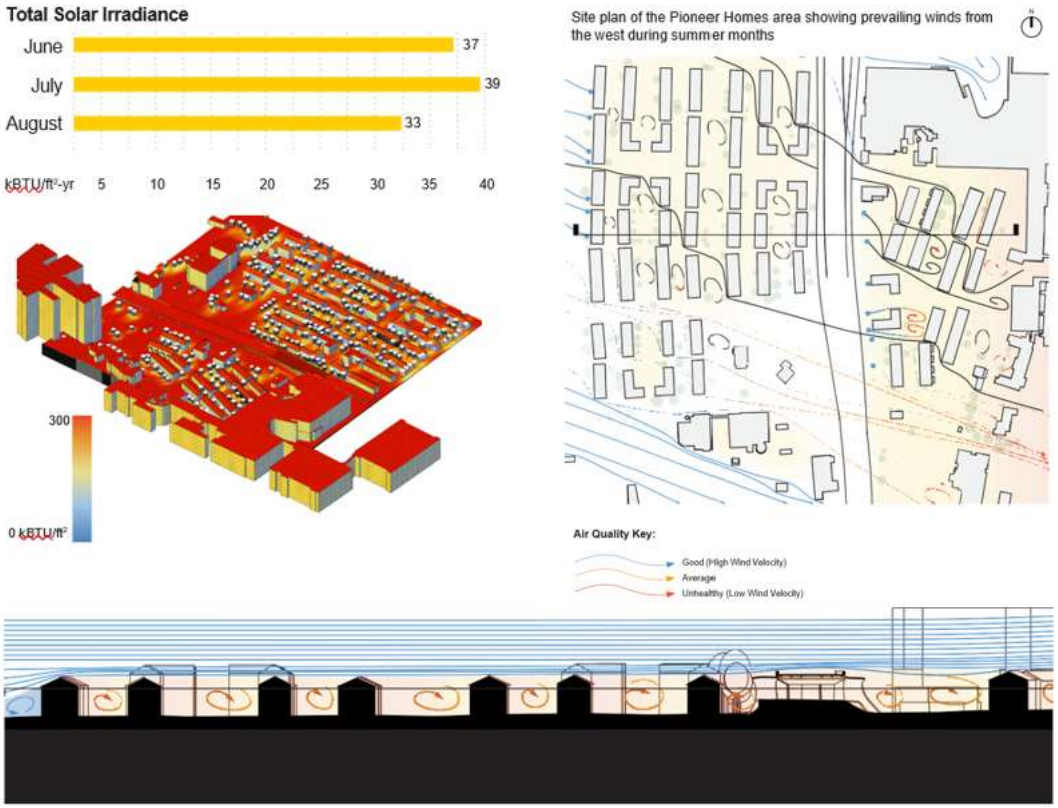

Figure 16. The existing thermal and air flow conditions in site 1.

Our analysis shows that solar radiation rates are very high for all buildings within site 1 (Fig. 16). As for air flow, the east-west site section shows skimming flow, where prevailing winds from the west during summer months do not circulate enough fresh air into spaces between buildings, often resulting in poor air quality sources for residences having a similar size and sufficiently close spacing.

Redesign plan: Configuration A

This configuration proposes a reduction in building density on the Pioneer Homes block by 25% in plan, and a replacement of 4-story buildings with 2-story building heights to reduce the ratio of building height to canyon width, which has been shown to improve fresh air circulation from the free stream in a Wake Interference or Isolated Roughness flow regime (van Moeseke et al., 2005). The north-south gaps between buildings were widened in this scheme to allow for greater cross- wind porosity admitting the westerly-northwesterly prevailing breezes during the hottest summer months when the site receives over 30 kBTU/ft2 -yr solar irradiance.

The reduced density and increased rugosity of surface area is expected to generate a variety of wake interference (with a canyon width to building height ratio of 1.5:1) and isolated roughness flow (with a canyon width to building height ratio of 3:1). This change could discernably reduce thermal intensity. Although air quality in spaces between the north-south running rows of buildings show the expected improvement in air circulation conditions, it becomes worse in others (Fig. 17).

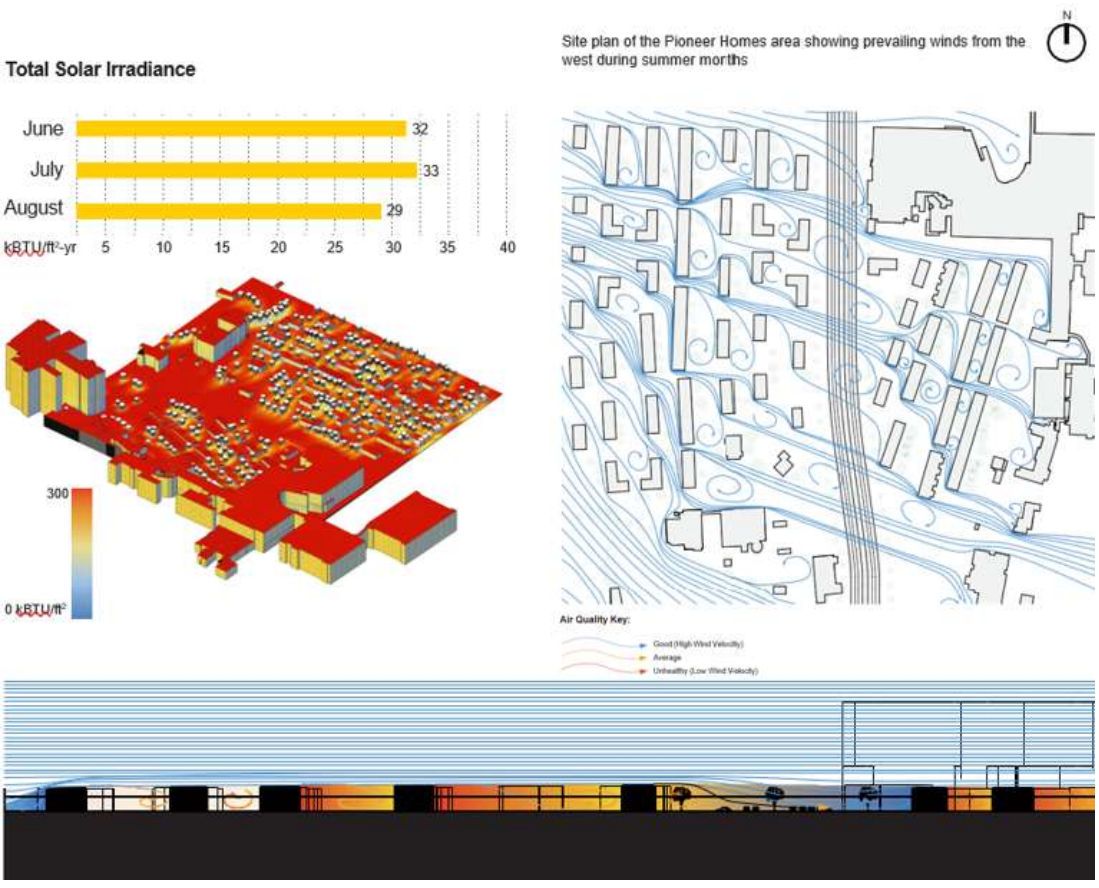

Figure 17. The results of configuration A in site 1.

Redesign plan: Configuration B

This proposed configuration scheme illustrates a modification in building rugosity in the proportion of building height regularity, thus changing the surface roughness of the landscape and altering the original skimming flow condition. Building heights are made to vary between two and four stories with the Pioneer Homes footprint used in Configuration A where density in plan view and west-to-east directional block porosity was reduced.

This redesign reduces density and increases rugosity of building surface area. Thus, it could significantly improve air quality in all spaces among buildings and maintain similar thermal results (Fig. 18).

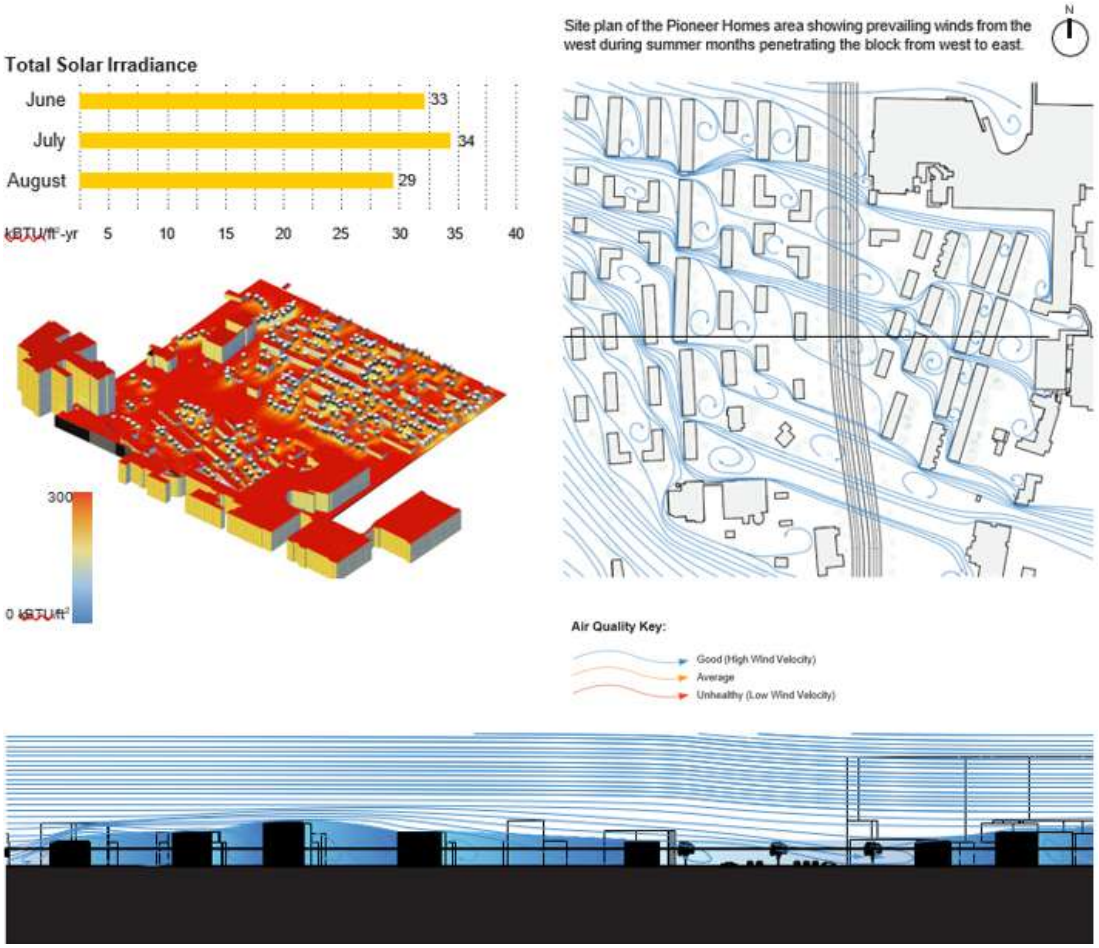

Figure 18. The results of configuration B in site 1.

Redesign plan: Configuration C

This configuration incorporates consideration towards the necessity of some low-income housing developments to maintain a minimum density of footprint to allow the inclusion of a higher number of units to meet community needs, while not exceeding district height restrictions. Here, all buildings have been represented at two stories in height (25 ft) with a staggered compact footprint to allow for light and pedestrian passageways between building rows. Given the higher density of this configuration, it is less likely to significantly improve air circulation conditions and air quality in the block than Configuration A or B, particularly between building rows where exterior air sources are relied upon for ventilation of residences in warmer months.

The results confirm the redesign expectation, which show limited improvement of air quality in some open spaces and a slightly improved thermal condition because staggering of row openings might allow for increased light penetration through the blocks (Fig. 19).

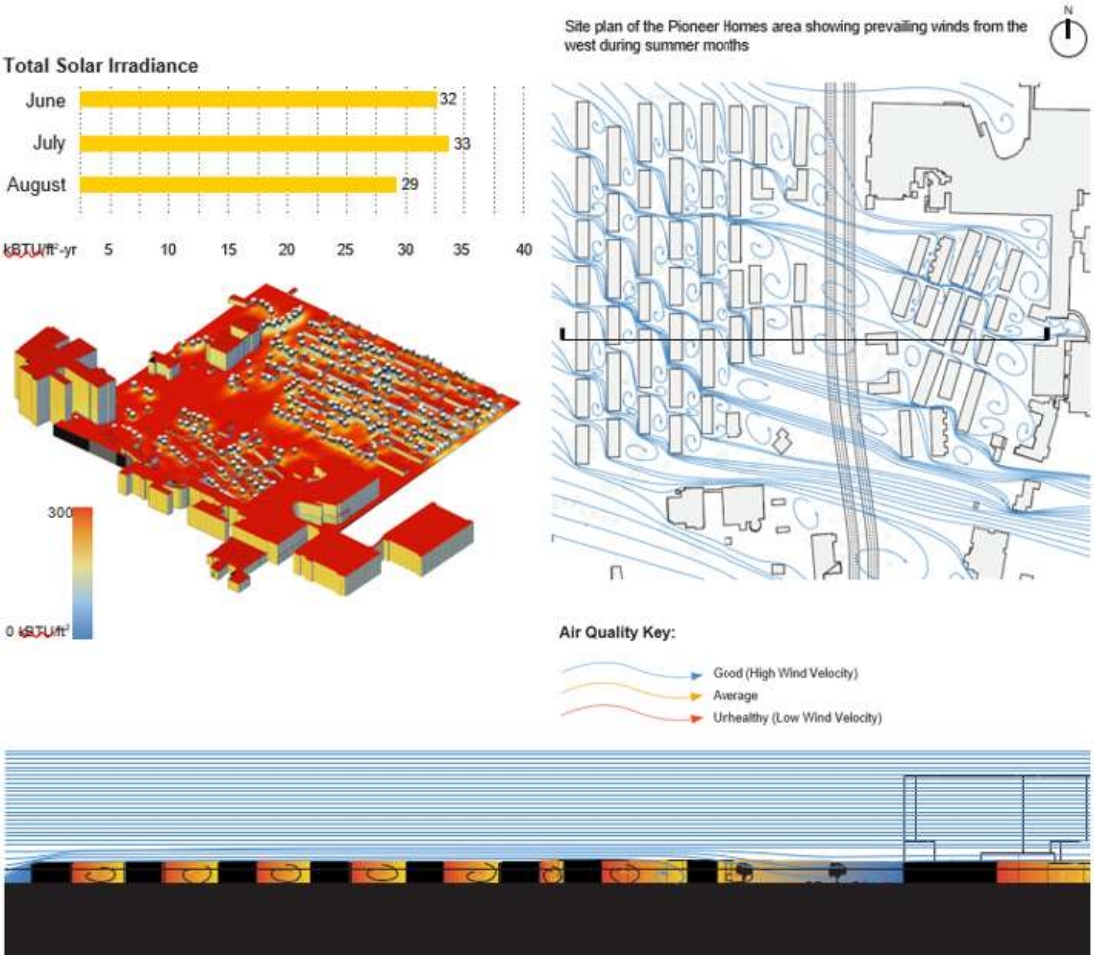

Figure 19. The results of configuration C in site 1.

Redesign plan: Configuration D

In Configuration D, density is once again considered, but building heights are staggered between two and four stories in the west-east direction, perpendicular to prevailing breezes, in order to increase site rugosity and attempt to reduce the effects of skimming flow typically found in arrangements having many rows of buildings of a very similar height. The circulation between buildings is expected to improve somewhat, but again not as significantly as seen in Configuration B. If housing development density must be maintained to a certain degree, other configurations of building mass might be investigated to enable sufficient access to fresh air and good cross-ventilation in naturally ventilated buildings lacking cooling systems.

This redesign increases variation in height that could somewhat mitigate skimming flow effects. Therefore, the results indicate that air quality in open spaces is generally improved at the degree close to Configuration B. Furthermore, the thermal condition could be improved even better than Configuration B (Fig. 20).

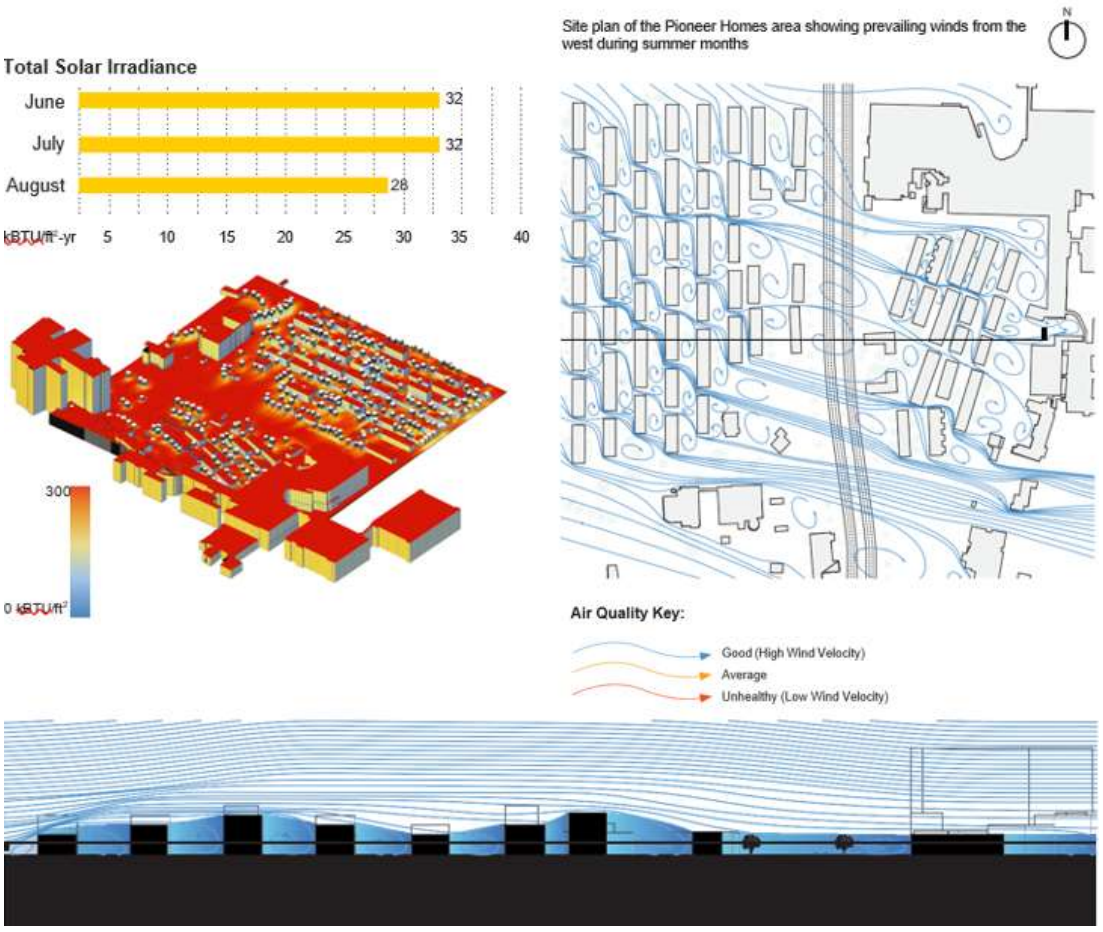

Figure 20. The results of configuration D in site 1.

Redesign plan: Configuration E

Configuration E tests the idea of subtracting staggered built areas within the densely-built housing block so that ventilation and occupied green spaces can contribute microclimatic benefits mitigating the Urban Heat Island conditions by cooling air and removing pollutants. Here, building heights are also varied between two and four stories to maintain the concept of rugosity and mitigate the effects of skimming flow. Though the overall footprint of the buildings is reduced by 12% on the block site, building heights can be increased and varied to make up for the loss of numbers of units. Configuration E is expected to improve airflow significantly through the creation of outdoor spaces or 'pocket parks' that reduce obstruction to effective airflow and reduce temperature locally, with the potential to improve air quality and thermal comfort especially with the inclusion of trees and other vegetation. The results show both the reduced thermal condition and improved air quality within the building blocks (Fig. 21).

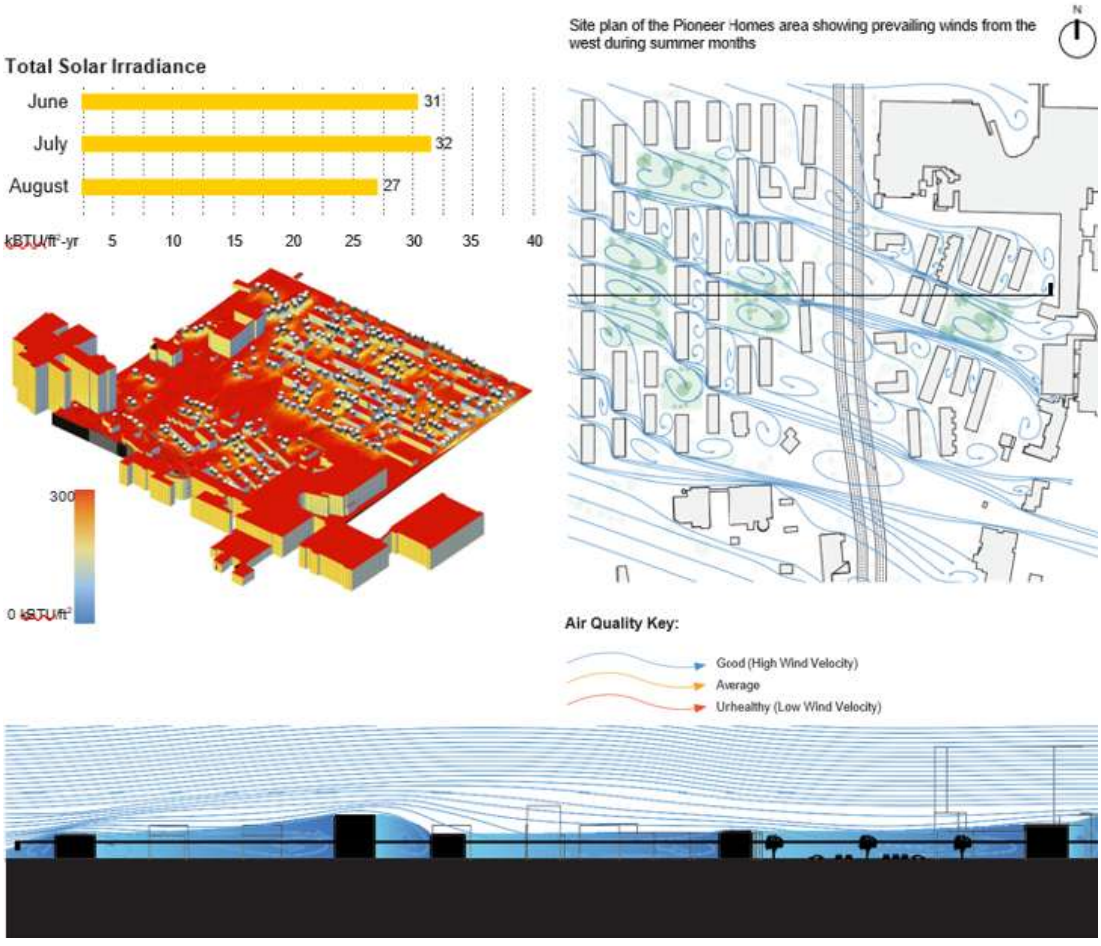

Figure 21. The results of configuration E in site 1.

3.3.2. Site 2: E Matson Ave

The E Matson Ave block, like Pioneer Homes, is located directly adjacent to the I-81 corridor. The block is bounded on the east by I-81 and a mass of vegetation, on the north by E Matson Ave, the west by S Salina St, and the south by Hobart Ave. Based on previous geospatial analysis at the CBG level, this site is distinct from site 1 in that it is in the CBG with statistically significant correlation between its poor socioeconomic status, reflected by the high composite index value and high simulated pollutant concentrations due to I-81 viaduct construction.

The west-to-east running Matson Ave block is in a Disadvantaged Community as defined by the New York State Energy Research and Development Authority and consists of closely-spaced light wood frame single family and multifamily homes of approximately 25’ – 30’ in height and between 1200 and 2400 SF having two stories, attics, and gable roofs (Fig. 22). The exceptions to this type on this block include 300-500 SF single-story storage sheds, garages, and dense masses of tree vegetation that range from 20’ to over 40’. The two northwest corner structures face west to S Salina St. In addition, there is an open paved lot where a one-story mechanic’s shop is sited at the southwestern corner of the block.

Figure 22. Typical Building Facades on Block.

As with the Pioneer Homes site, the focus for the second site is on the block’s air quality for natural ventilation and outdoor thermal comfort, both of which predominate in the warmer months, so the focus of the environmental analysis and proposed alternatives will be on the summer period whose wind pattern is shown in Figure 23.

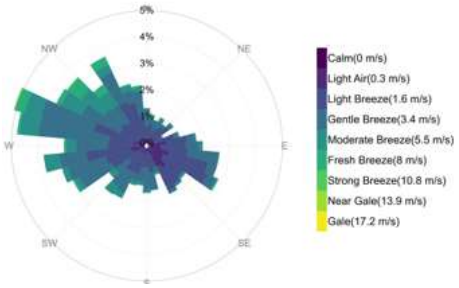

Figure 23. The wind pattern in summers

In the existing condition, narrow spacing between buildings having the same or similar height can potentially result in skimming flow once again. It is possible that traffic pollutants from the nearby I-81 corridor and the busy S Salina St could both be conveyed into this block with the result of poor air quality and poor indoor and outdoor thermal comfort, indicators which are associat- ed with low-income communities and experiencing ill effects from environmental hazards such as those concomitant with climate change.

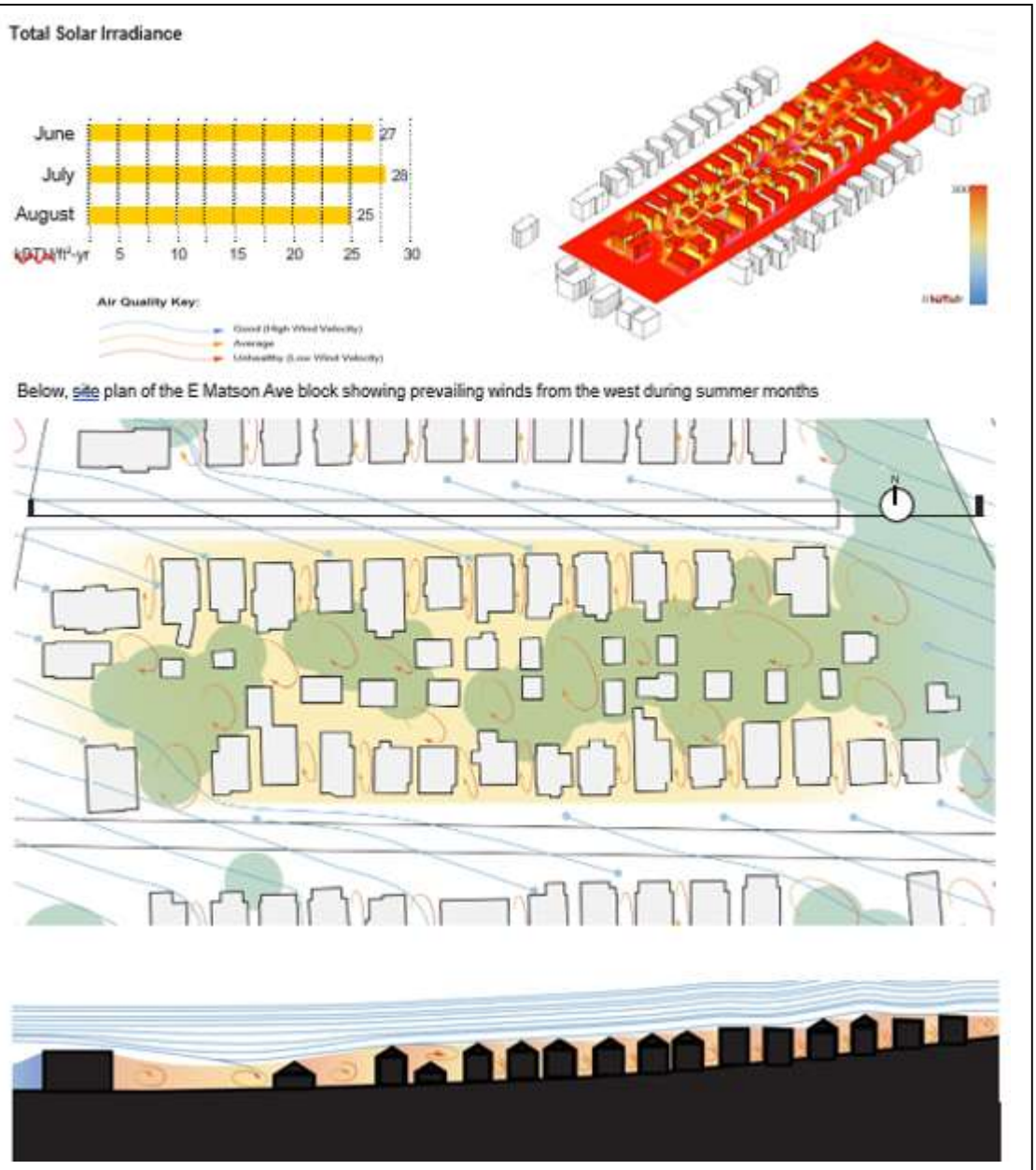

Figure 24. The existing thermal and air flow conditions in site 2.

Our analysis shows that east-west site section is dominated by skimming flow in which prevailing winds from the west during summer months do not circulate enough fresh air into spaces between buildings. This often results in poor air quality sources for residences and outdoor occupied spaces (Fig. 24).

Redesign plan: Configuration A

This proposed configuration reduces the built density of the block by reducing the footprint of the buildings to facilitate the passage of fresh air in between horizontal rows of buildings. Such a reduction of footprint would result in housing of a smaller scale, and thus may be suited to smaller-size families or single residents as part of future developments. Maintaining setbacks toward each property's street frontage, this arrangement effectively increases the size of each privately-owned yard and aggregates central green space, possibly enabling the effect of a stronger microclimate such as we see in urban park spaces. With the housing type seen on this block, many window openings are found on the west and east walls, and most buildings do not have central cooling systems, with few having portable window air conditioning units for a few rooms. Such an arrangement indicates the requirement for fresh air to enter on either side of the residential buildings, as well as from the north and south. Configuration A, therefore, may not be sufficient in this block's context to ensure fresh air access or improve other index parameters.

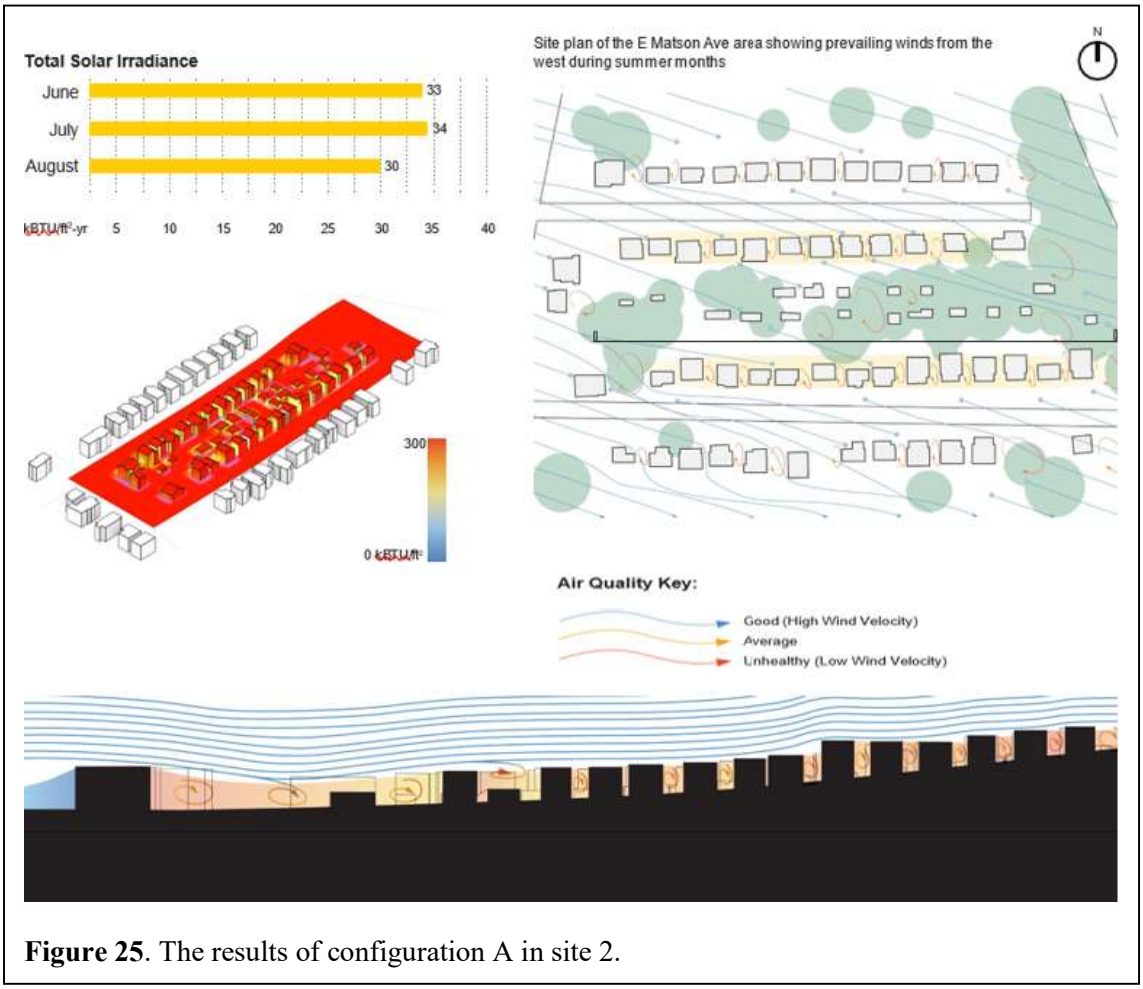

Figure 25. The results of configuration A in site 2.

In this configuration, due to the unchanged narrow spacing between buildings from west to east (parallel with the avenues), there may still be poor circulation between buildings along that axis (see the block-scale section in Fig. 25).

Redesign plan: Configuration B

In Configuration B, the original two rows of buildings were consolidated into a single row running in the west-to-east direction and displacing the original street-adjacent volumes of housing with green space to allow open access to ventilation to a greater exterior area of the buildings (the right side of Fig. 26). This configuration reduces the built area by approximately 50%, but does not increase the height of the buildings to compensate for lost leasable residential area. While there is greater exterior envelope area exposed in this configuration, the spacing along the west-east axis is still very small between the buildings, ranging from a width to height ratio of between 0.5:3 to 1:3. If airflow is channeled in between the smaller spaces in a north-south direction, then the close spacing may result in local higher-velocity flow due to the Venturi effect. Examination of the Syracuse wind rose data, however, indicates that direct north wind is less common than wind coming from the west-northwest direction. In this case, therefore, with a reduction in density, the design recommendation would be to stagger the buildings along the west-east axis to render a higher-porosity aggregation of solid forms perpendicular to the prevailing breeze. The results confirm that though good circulation may be in effect to the north and south of this centralized row of buildings, poor air quality may still prevail in some locations in the building given the close spacing.

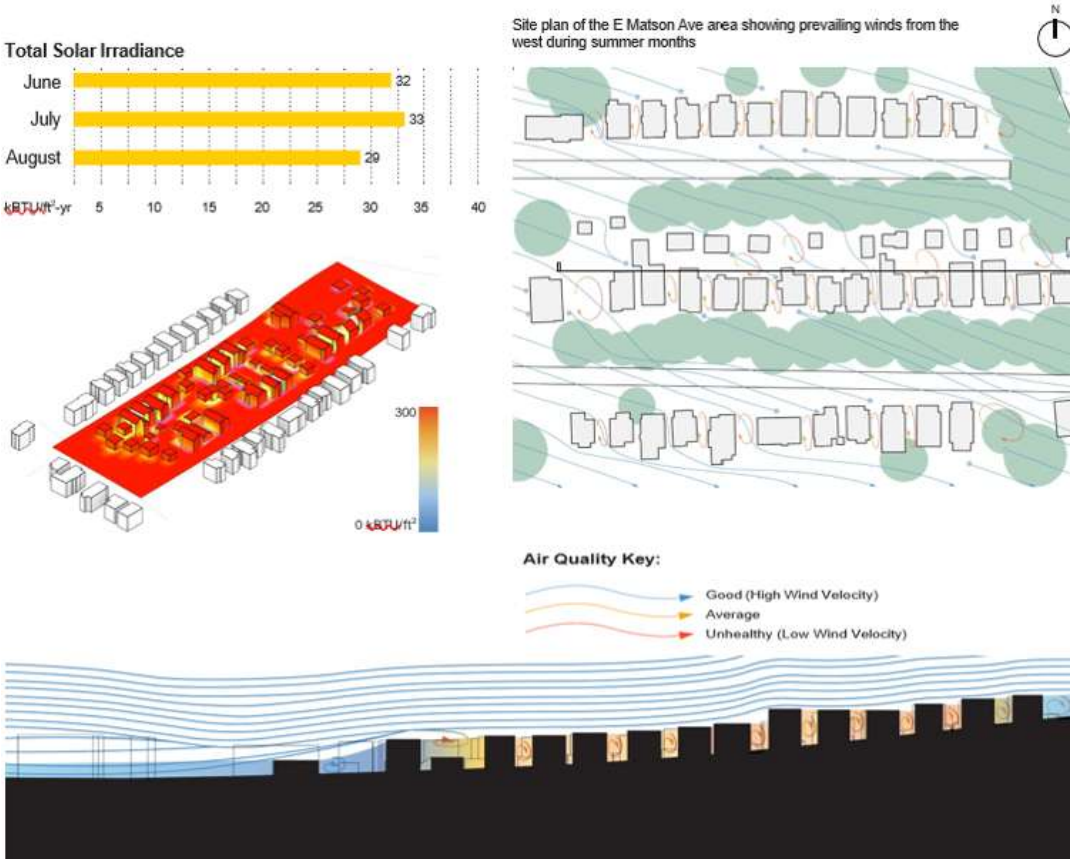

Figure 26. The results of configuration B in site 2.

Redesign plan: Configuration C

Configuration C introduces greater porosity into the densely-built block along the west-east axis to facilitate the admission of fresh airflow in between the buildings. Instead of two contiguous rows, clusters are formed with green space of a width equivalent to three buildings in an arrangement that could result in Isolated Roughness or Wake Interference flow between clusters. Between individual buildings, however, the original spacing remains close and could continue to result in pockets of recirculating air and possible poor air quality. To improve spatial quality and access to fresh air, providing more space between clusters of buildings is adopted in conjunction with the design of all façades with openings that are relied upon for ventilation.

The results display some improvement of air quality. Particularly, the wake interference and isolated roughness flow regimes shown in the east-west site section (the bottom of Fig. 27) indicate that prevailing winds from the west during summer months could result in good circulation of fresh air between clusters of buildings, but possibly less so between individual buildings within a cluster.

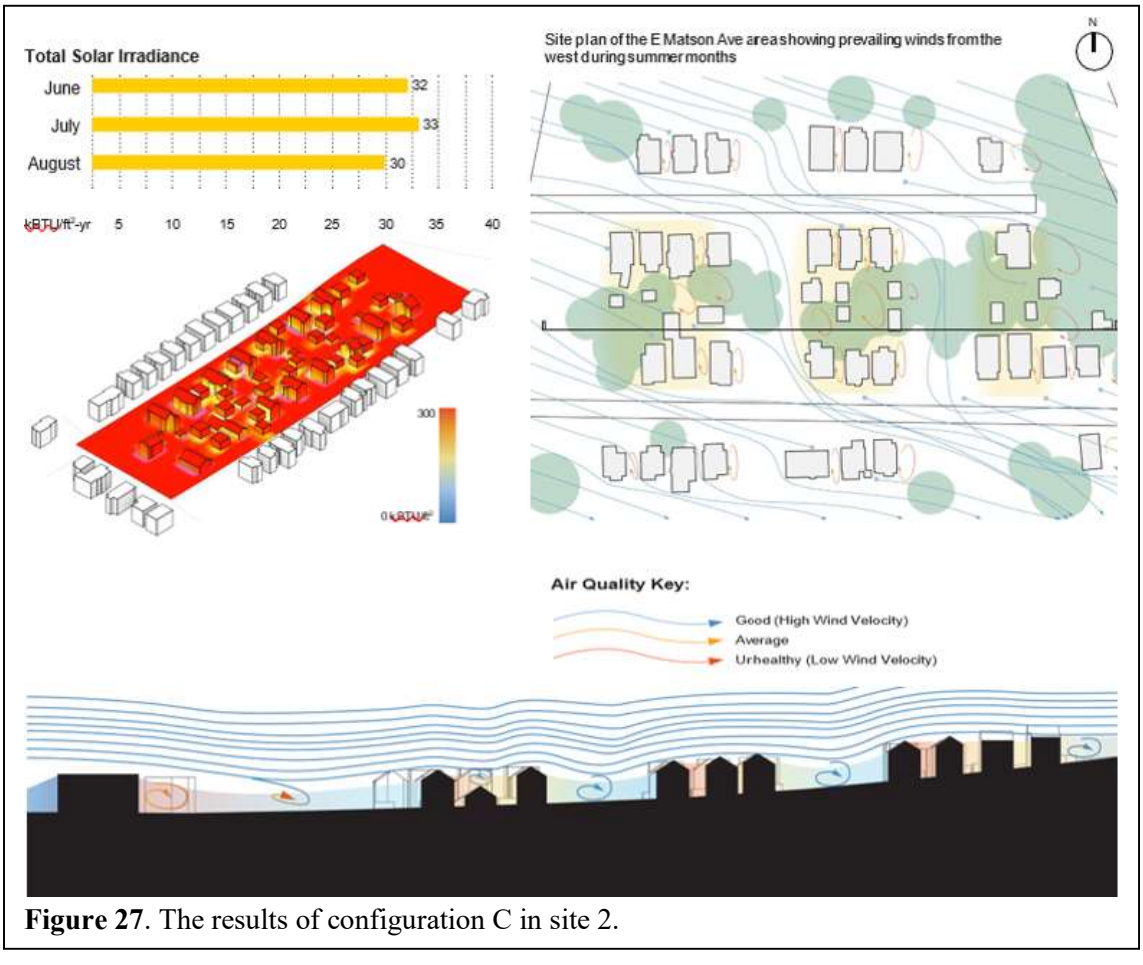

Figure 27. The results of configuration C in site 2.

Redesign plan: Configuration D

In Configuration D, the buildings are once again organized into clusters, but the clusters are grouped in an alternating pattern from west to east along the primary block axis so that wind directions not having a cardinal orientation directly from north, south, east, or west can circulate through the block. In addition, clusters of green space and vegetation are positioned to improve the ability of cooling microclimates to function during hot weather and provide quality outdoor space, which is correlated with improved occupant wellbeing. A reduction in impermeable built surface increases the site's ability to hold stormwater, which can mitigate the risks of flash flooding during heavy rains which Syracuse often experiences in the summer season. This design configuration thus far provides the most individual and community health benefits for the site while considering the need for a certain amount of density or a minimum number of units per block.

The results (Fig. 28) show that between clusters Isolated Roughness flow can potentially predominate, but in spaces between the buildings of dense clusters, the height of the buildings precludes sufficient circulation of fresh air. The air quality is greatly improved in this configuration.

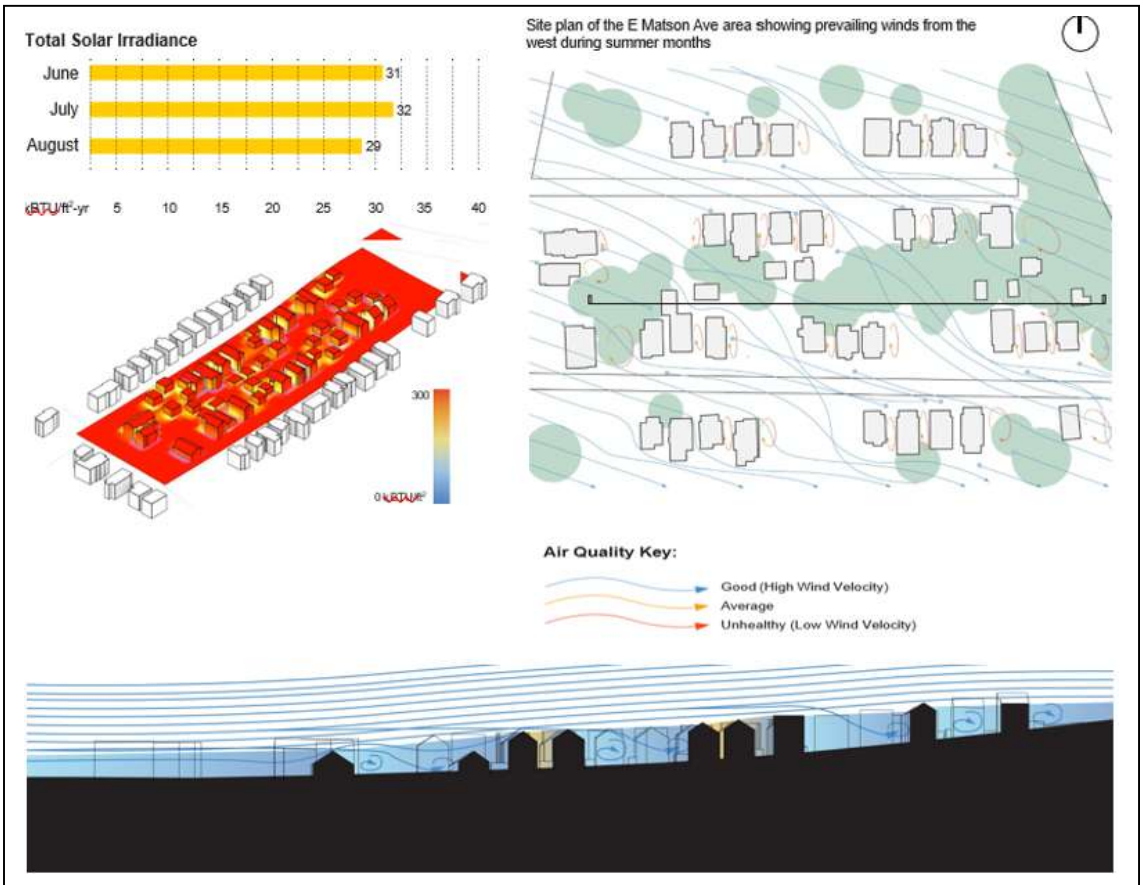

Figure 28. The results of configuration D in site 2.

Redesign plan: Configuration E

Configuration E reduces the block density by utilizing only 50% of the building footprints of the original scheme, so that increased areas of green space lie directly adjacent to the buildings on all sides. This scheme improves upon Configuration D by increasing the spacing between buildings in the east-west direction along the primary block axis to admit prevailing summer breezes. Based on the proportions between the spacing and the building height, Wake Interference flow and Isolated Roughness flow can predominate where airflow encounters buildings, and between buildings, greatly increased porosity can admit fresh air into and through the entirety of the block. In this configuration, the amount of green space with mature tree cover is sufficient to affect the microclimate and potentially result in cooling of local airflow for improved thermal comfort in exterior and interior spaces.

The results show that the site now has greatly expanded green outdoor spaces. This change allows substantial fresh airflow into spaces between buildings as demonstrated in wake interference and isolated roughness flow along the east-west site section (the bottom of Fig. 29). The only poor air quality is assumed in the rear of the commercial auto shop, shown left, which may have some local undesired downwind effects. Overall, air quality of the site could be greatly improved in this configuration,

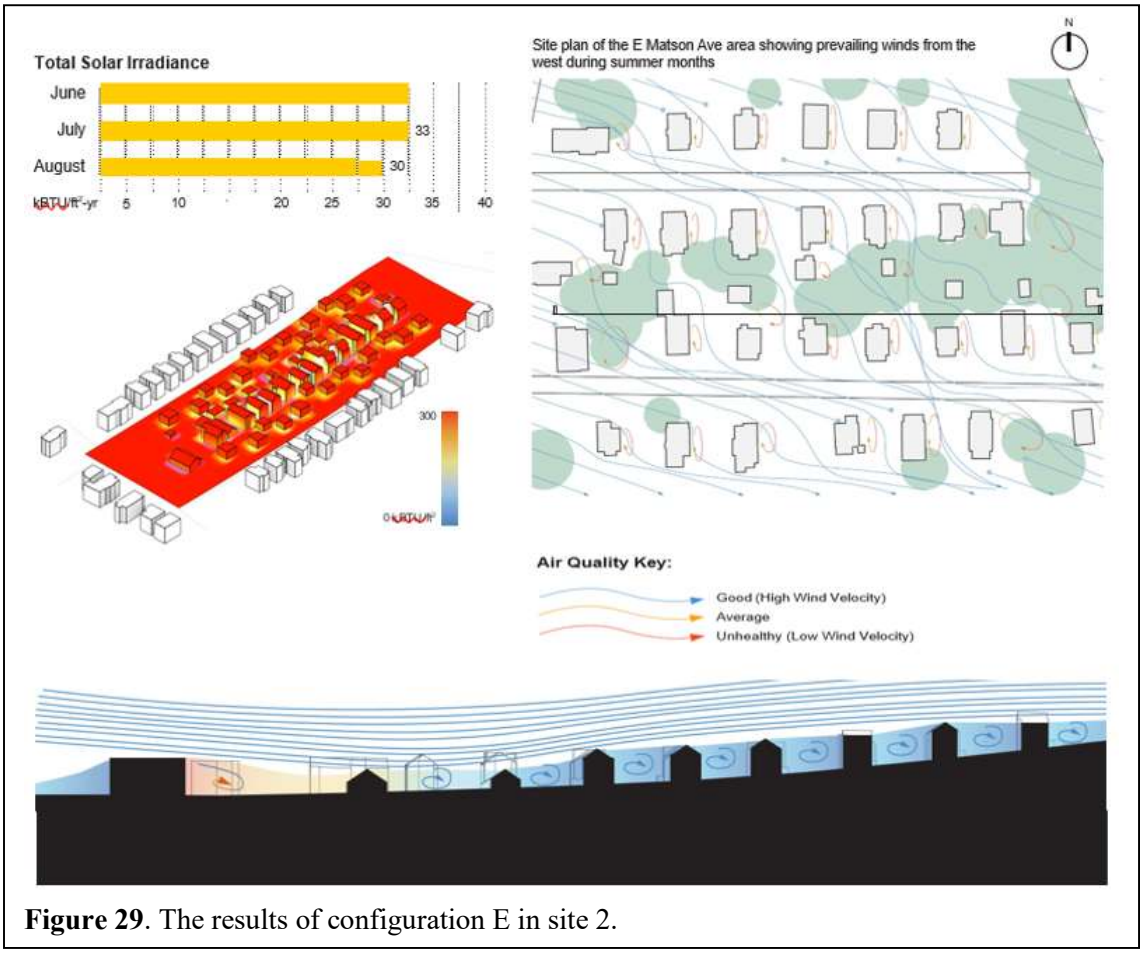

Figure 29. The results of configuration E in site 2.

3.3.3. Comparison of redesign effects between the two sites

The two sites analyzed share both geospatial and morphological similarities as well as key differences that influence the nature and significance of the impact resulting from morphological changes in building form, spacing, and configuration. While both sites were classified as suffering moderate degrees of air pollution and higher percentage of disadvantaged populations, only the second site analyzed at E Matson Ave shows a strong correlation between degree of air pollution and percentage of disadvantaged population with statistical significance. For other sites in Syracuse having similar urban contexts, including geospatial and morphological characteristics to those of the E Matson Ave block, it may be inferred that a strong correlation between the two factors (of pollution and disadvantaged population) would be found.

For the first site at Pioneer Homes, a multifamily low-rise typology was studied in a series of alternative configurations of building geometries and introducing varying spacing between buildings to allow pathways for higher-velocity fresh air to enter and disrupt recirculating urban vortices in a comparatively dense development. These measures qualitatively demonstrate potential improvements in air quality with accompanying benefits of possible microclimate cooling with the integration of green space and vegetation adjacent to windows upon which many residents rely for natural ventilation in the summer months. Improved thermal comfort for outdoor space and air supply, along with improved air quality, are associated with better health and wellbeing outcomes, and can contribute to community resilience against the ill effects of heat stress and pollution.

The second site at E Matson Ave represents a less dense typology more typical of early 20th-century suburban housing settlements. Though many of the houses are multifamily, they are of light wood frame construction with gabled roofs and consistent privately-owned open or green space allocated per structure in the form of yards, setbacks, and circulation access. Because of this less-dense configuration with green space already integrated, the set of alternative configuration strategies implemented in Pioneer Homes were shown to have a ***lesser*** impact on the admission of fresh air into the site. With the measures examined, however, including the introduction of alternative spacing and the interspersing of larger areas of green space and vegetation between buildings, some degree of microclimate cooling could be enabled to cool the air circulating in outdoor spaces, particularly between buildings where poor circulation was likelier but fresh air was needed for ventilation during summer periods. For this site, the substantially lessened density could potentially result in a financially infeasible reduction of the number of units on the block.

It should be noted that several considerations that would be incorporated for a full design process with community stakeholder input have been omitted here for the purpose of the present study, but this design and analysis step is critical to test morphological and massing concepts to demonstrate the potential environmental and energy advantages to clients and occupants during design review. In the context of this step, however, consisting of alterations in building geometry and site morphology, the compounding measures of increasing site porosity in the direction of prevailing seasonal airflow, integrating microclimate cooling, and reducing density

have greater potential to improve factors relating to comfort, health, and wellbeing of occupants at high-density urban sites. As seen in Pioneer Homes, if scaled and implemented in aggregate on a number of sites, there is the potential with such design measures to improve community resilience and mitigate the effects of heat stress and reduce exposure to pollutants.

4. Discussion

4.1. A Community-Centered Multidisciplinary Framework

The I-81 viaduct project inevitably produces additional sources of air pollution that adversely affect the well-being of local residents in Syracuse. Identifying vulnerable populations who may suffer most from elevated air pollution due to highway construction is challenging but critical for developing effective mitigation strategies. This study demonstrates that our novel approach can successfully achieve this identification while offering appropriate design solutions for policy development.

Our approach effectively integrates air pollution modeling and GIS-based geospatial analysis with architectural design, highlighting the value of multidisciplinary collaboration among engineers, geographers, and architects. The fundamental nature of this approach is that it constitutes community-focused research operating at an intermediate spatial scale, the meso scale (Batty, 2008), specifically using census block groups (CBGs) rather than analyzing entire cities (coarser scale) or individual buildings (finer scale).

By aggregating data at the CBG level, we can supply CBG-level porosity data for porous medium CFD models to predict pollutant concentrations across the entire city. This method enables efficient, large-scale simulations that can be performed in near real-time. At this spatial resolution, predicted pollution data can be directly linked to various social determinants of public health relevant to air pollution, including through geographically weighted regression (GWR) modeling. These geospatial analyses enable development of maps indicating spatially variable CBGs that may experience high degrees of environmental injustice from elevated air pollution due to highway construction. These maps provide essential background information for subsequent architectural design interventions and associated impact analyses.

The success of this approach relies on quantitatively linking social and environmental characteristics of communities through data aggregated at the CBG level. This methodology demonstrates significant potential for application to other cities facing similar urban environmental challenges.

4.2. Limitations

However, this study has several limitations primarily due to time constraints. These limitations are described as follows:

4.2.1. Improving CFD Modeling Accuracy

When comparing predicted pollutant concentrations with field-measured values at existing sampling sites along the I-81 viaduct, we observed that predicted values were consistently lower than measured ones by more than 10 times. Importantly, this significant discrepancy occurred across all predicted values, suggesting that (i) systematic errors exist in the model structure, and (ii) these errors do not alter the spatial pattern

characteristics of predicted pollutant concentrations. Therefore, the subsequent geospatial analyses remain robust. However, identifying the causes of these systematic errors and correcting them in future model simulations is essential.

Additionally, two GIS-based model input datasets require improvement. First, the key input parameter of porosity was calculated based on the proportion of open spaces in each CBG. This calculation assumes buildings within each CBG have similar heights, thereby ignoring the potentially significant impact of variable building heights and their spatial variations. Future work should employ a different urban form parameter, rugosity, which specifically accounts for individual building heights. Second, the street network used as the fundamental model structure is currently treated uniformly across the city. Since streets serve as pathways for airflow in urban environments, it is crucial to distinguish different street types based on their widths. We believe that utilizing accurate street network data could substantially improve model prediction accuracy.

4.2.2. Enhancing Geospatial Analysis Methodology

In geospatial science, no established theory exists to determine which geostatistical tools or geospatial techniques should be employed for specific analyses. This is why geospatial analysis is often characterized as exploratory data analysis. This study identifies three key issues that require further investigation.

First, the selection of the four social determinants of public health was primarily based on our understanding of their general roles in public health outcomes. Future research should explore additional variables that may be relevant to air pollution vulnerability, potentially including factors such as access to healthcare, housing quality, or proximity to green spaces.

Second, combining the four selected variables into a single composite index represents a novel approach in this study, effectively addressing the statistical constraints of performing GWR modeling analysis related to sample size limitations. However, alternative methods for combining these variables exist, introducing uncertainties associated with the weighted linear aggregation model employed in this research. Future work should test different combination methodologies to assess the robustness of our composite index approach.

Third, the GWR analysis utilized annually averaged predicted pollutant concentrations derived from 12 months of data to obtain the spatial distribution of air pollution. This approach inevitably neglects the potential impact of seasonal variations in air pollution on GWR results. To improve modeling accuracy, future research will employ time-series GWR models to identify more precise temporal correlations and capture seasonal dynamics in the relationship between air pollution and social vulnerability.

4.2.3. Advancing Community Design Analysis

While we successfully demonstrated air quality improvements at varying degrees across different redesign scenarios, our results remain primarily qualitative. More robust modeling-based analysis is needed to quantify the extent to which air quality in selected community blocks could be improved, providing stronger guidance for future community grid design following I-81 viaduct removal.

Future design strategies should be grounded in the hierarchical structure of spatial units adopted by the US Census Bureau (USCB), which encompasses census blocks, census block groups, and census tracts from small to large scales. A significant advantage of aligning design sites with these spatial units is that design analysis results can be directly linked to spatially aggregated building typologies and socioeconomic conditions of neighborhoods, the data that are largely unavailable at finer spatial scales (e.g., individual households).

Furthermore, community design analysis aligned with USCB spatial units can leverage results from our ongoing research examining urban morphology impacts on microclimate. For instance, we have calculated six parameters representing various three-dimensional spatial properties of buildings within each of Syracuse's 133 CBGs. For each architectural design scenario at the CBG level, we can recalculate these parameters and quantitatively demonstrate how the spatial characteristics of buildings within the redesigned CBG have changed.

By combining our urban morphology analysis with the potential for upscaling modeling analysis using packages such as ENVI-Net, we can provide more robust and efficient planning options for policymakers. This integrated approach would enable quantitative assessment of design interventions while maintaining direct connections to both environmental outcomes and community characteristics.

5. Conclusions and Recommendations

This project developed a novel interdisciplinary approach that integrates concepts and techniques from environmental engineering (air pollution modeling), geography (geospatial analysis), and architecture (community design and analysis). Using this approach, we successfully achieved the proposed research goal by developing a comprehensive framework for identifying neighborhoods most vulnerable to air pollution and experiencing elevated pollution levels from I-81 viaduct construction.

By integrating air pollution modeling with GIS-based geospatial analysis and coupling these outcomes with subsequent architectural design interventions, this framework enabled us to accomplish the following three objectives:

(1) By dividing the Syracuse city area into 133 census block groups (CBGs) and incorporating the surrounding street network using GIS techniques, we successfully developed a porous-medium CFD model for predicting air pollution concentrations across the entire city. The model utilizes porosity as the key input parameter, determined as a single value representing buildings within each CBG. This upscaled CFD model can predict spatially variable air pollutant concentrations throughout Syracuse. Combined with wind pattern data, the model effectively predicts spatial patterns of air pollution concentrations and their annual variations. These modeling outcomes can be readily integrated into the ArcGIS platform, enabling direct linkage between spatially variable air pollution conditions and the socioeconomic status of local communities.

(2) Through geospatial analysis, we developed a comprehensive index that reflects the spatial distribution of socioeconomic status of local communities at the CBG level. This index effectively captures the collective effects of four individual social determinants of public health relevant to air pollution: poverty, vulnerability to air pollution, segregation, and distance to medical resources. By comparing the spatial distribution of this index with predicted annually averaged pollutant concentrations, we identified local neighborhoods (represented by CBGs) that are both vulnerable to air pollution and likely to experience severe air pollution from I-81 viaduct construction. Our GWR modeling analysis further revealed communities with statistically significant correlations between the index and predicted pollutant concentrations, suggesting that air pollution conditions in these areas may be a primary driving force influencing the existing socioeconomic status of these communities. Notably, we found that most of these vulnerable communities are located along the I-81 viaduct corridor. This finding suggests that Syracuse's wind patterns facilitate the concentration of elevated air pollution from I-81 viaduct construction within the highway corridor, causing neighborhoods in this area to suffer disproportionately from elevated air pollution exposure.

(3) We investigated potential redesign strategies for affected local communities from an architectural perspective. Using the map identifying vulnerable communities (CBGs) most affected by elevated air pollution, we selected two sites along the I-81 viaduct representing two different CBGs: one without a statistically significant correlation between the composite index and predicted elevated air pollutant concentrations, and another with such a correlation. By analyzing airflow patterns and thermal conditions across five different design scenarios and comparing them with original community settings, we demonstrated that varying degrees of improvement in air quality and thermal conditions could be achieved. The improvements were more pronounced at the site showing significant correlation between the two variables, suggesting that targeted architectural interventions may be more effective in communities where air pollution serves as a primary driver of socioeconomic vulnerability.

Our results provide valuable insights into the spatial characteristics of elevated air pollution from I-81 viaduct construction and identify planning design strategies that could most effectively improve the socioeconomic status of affected local communities. In the near future, we will develop this framework into an analytical tool that can be applied to other aspects of public health and adapted for use in other cities facing similar infrastructure-related environmental challenges.

6. References

Adolphe, L. (2001). *A Simplified Model of Urban Morphology: Application to an Analysis of the Environmental Performance of Cities*. *Environment and Planning B: Planning and Design*, *28*(2), 183–200. https://doi.org/10.1068/b2631

Antonioni, Giacomo, et al. (2012). *Comparison of CFD and operational dispersion models in an urban-like environment. Atmospheric Environment* 47, 365-372.

Batty, M. (2008). *The Size, Scale, and Shape of Cities. Science*, 319(5864), 769–771. https://doi.org/10.1126/science.1151419.

Chen, Y., Hu, Z., Bai, H., and Shen, W. (2022). *Variation in Road Dust Heavy Metal Concentration, Pollution, and Health Risk with Distance from the Factories in a City-Industry Integration Area, China. Int J Environ Res Public Health*, *19(21)*, 14562. doi: 10.3390/ijerph192114562.

Clark, L.P., Millet, D.B., and Marshall, J.D. (2014). *National Patterns in Environmental Injustice and Inequality: Outdoor NO_2 Air Pollution in the United States*. *PLOS ONE* 9(4): e94431. https://doi.org/10.1371/journal.pone.0094431.

Essamlali, I., Nhaila, H., & Khaili, M. E. (2025). *Impact of urban block shape on traffic and air quality: A SUMO-based comparative study of rectangular, radial, and triangular forms. Transportation Research Interdisciplinary Perspectives*, 31, 101413. https://doi.org/10.1016/j.trip.2025.101413.

Fotheringham, A. S., Brunsdon, C., and Charlton, M. (2002). *Geographically Weighted Regression: The Analysis of Spatially Varying Relationships.* Wiley.

Hassan, A. M., ELMokadem, A. A., Megahed, N. A., & Abo Eleinen, O. M. (2020). *Urban morphology as a passive strategy in promoting outdoor air quality. Journal of Building Engineering*, 29, 101204. https://doi.org/10.1016/j.jobe.2020.101204

Giovannini, L., Ferrero, E., Karl, T., Rotach, M. W., Staquet, C., Trini Castelli, S., and Zardi, D. (2020). *Atmospheric Pollutant Dispersion over Complex Terrain: Challenges and Needs for Improving Air Quality Measurements and Modeling*. *Atmosphere*, *11*(6), 646. https://doi.org/10.3390/atmos11060646.

Hoek, G., Krishnan, R.M., Beelen, R., Peters, A., Ostro, B., Brunekreef, B,, and Kaufman, J.D.. (2013) *Long-term air pollution exposure and cardio- respiratory mortality: a review. Environ Health*, 12(1):43. doi: 10.1186/1476-069X-12-43. PMID: 23714370; PMCID: PMC3679821.

Jargowsky, P.A. (2015). *Architecture of segregation: Civil unrest, the concentration of poverty, and public policy*: The Century Foundation https://tcf.org/content/report/architecture-of-segregation/.

Kaveh, S., Habibi, A., Nikkar, M., & Aflaki, A. (2024). *Optimizing green infrastructure strategies for microclimate regula- tion and air quality improvement in urban environments: A case study. Nature-Based Solutions*, 6, 100167. https://doi. org/10.1016/j.nbsj.2024.100167.

Lane, S. (2015). *Why Are Our Babies Dying?* Routledge, New York.

Liu, W., Huang, Z., Cui, D., Ma, D., Mei, S., & Guo, R. (2025). *Impact of street interface permeability on ventilation and pollutants dispersion in urban street spaces. Building and Environment*, 274, 112779. https://doi.org/10.1016/j.build-env.2025.112779.

Makvandi, M., Yuan, P. F., Ji, Q., Li, C., Elsadek, M., Li, W., Hassan, A., & Li, Y. (2024). *Resilience to climate change by improving air circulation efficiency and pollutant dispersion in cities: A 3D-UFO approach to urban block design. Heliyon*, 10(17), e36904. https://doi.org/10.1016/j.heliyon.2024.e36904.

Malczewski, J. (1999). *GIS and Multicriteria Decision Analysis.* Wiley. https://www.wiley.com/en-us/GIS+and+Multicriteria+Decision+Analysis-p-9780471329442.

Pantusheva, Mariya, et al. (2022). *Air pollution dispersion modelling in urban environment using CFD: a systematic review*. *Atmosphere*, 13.10, 1640.

Pope, C.A. and Dockery, D.W. (2006) *Health Effects of Fine Particulate Air Pollution: Lines that Connect. Journal of the Air & Waste Management Association*, 56, 709-742. http://dx.doi.org/10.1080/10473289.2006.10464485.

Wang, Y., Zhong, K., Cheng, J., Xu, J., He, J., & Kang, Y. (2025). *Numerical investigation of building gap effects on traffic pollutant dispersion in urban networks with intersecting streets*. *Atmospheric Pollution Research*, 16(6), 102475. https://doi. org/10.1016/j.apr.2025.102475.

Wang, Y., Zhong, K., He, J., Cheng, J., Qi, M., & Kang, Y. (2025). *Impacts of pollution from surrounding street canyons on air cleanliness in urban ventilation corridors. Sustainable Cities and Society*, 130, 106552. https://doi.org/10.1016/j. scs.2025.106552.

Wu, Z., Lin, T., Li, Z., Li, Y., Guo, T., and Guo, Z. (2017). *Atmospheric occurrence, transport and gas–particle partitioning of polychlorinated biphenyls over the northwestern Pacific Ocean, Atmospheric Environment, 167*, 487-495. https://doi.org/10.1016/j.atmosenv.2017.08.056.

Yu, C., Deng, Y., Qin, Z., Yang, C., and Yuan, Q. (2023). *Traffic volume and road network structure: Revealing transportation-related factors on PM2.5 concentrations, Transportation Research Part D: Transport and Environment, 124*, 1361-9209 doi.org/10.1016/j.trd.2023.103935.

Yu, X., & Ma, J. (2025). *Mapping the distribution of pedestrian exposure to air pollution on urban road segments based on mobile monitoring and street view images. Applied Geography*, 179, 103644. https://doi.org/10.1016/j.apgeog.2025.103644.